NAVAL POSTGRADUATE SCHOOL

Monterey, California

THESIS

AN ASSESSMENT OF THE POTENTIAL ROLE OF MULTISPECTRAL IMAGERY IN BATHYMETRIC CHARTING

by

Richard Thomas Joy

September 1984

Thesis Advisor: James L. Mueller

Approved for public release; distribution unlimited

REPORT DOCUMENTATION PAGE

READ INSTRUCTIONS BEFORE COMPLETING FORM

1. REPORT NUMBER

2. GOVT ACCESSION NO.

3. RECIPIENT'S CATALOG NUMBER

4. TITLE (and Subtitle)
An Assessment of the Potential Role of Satellite Multispectral Imagery in Bathymetric Mapping

5. TYPE OF REPORT & PERIOD COVERED
Master's Thesis
September 1984

6. PERFORMING ORG. REPORT NUMBER

7. AUTHOR(s)
Richard Thomas Joy

8. CONTRACT OR GRANT NUMBER(s)

9. PERFORMING ORGANIZATION NAME AND ADDRESS
Naval Postgraduate School
Monterey, California 93943

10. PROGRAM ELEMENT, PROJECT, TASK AREA & WORK UNIT NUMBERS

11. CONTROLLING OFFICE NAME AND ADDRESS
Naval Postgraduate School
Monterey, California 93943

12. REPORT DATE
September 1984

13. NUMBER OF PAGES
97

14. MONITORING AGENCY NAME & ADDRESS(if different from Controlling Office)

15. SECURITY CLASS. (of this report)
UNCLASSIFIED

15a. DECLASSIFICATION/DOWNGRADING SCHEDULE

16. DISTRIBUTION STATEMENT (of this Report)

Approved for public release, distribution unlimited

17. DISTRIBUTION STATEMENT (of the abstract entered in Block 20, if different from Report)

18. SUPPLEMENTARY NOTES

19. KEY WORDS (Continue on reverse side if necessary and identify by block number)
Satellite bathymetry, multispectral imagery, Landsat, Multispectral Scanner (MSS), remote sensing, bathymetric chart revision, Great Bahama Bank, West Florida Shelf.

20. ABSTRACT (Continue on reverse side if necessary and identify by block number)
Previous research has demonstrated the feasibility of deriving water depth information from Landsat Multispectral Scanner (MSS) digital data. However, previously published results, analysed together with two new case studies, show that the magnitude of errors (approximately 1-2 meters) in MSS single-band depth extimates is too large for direct production of bathymetric charts. Better accuracy is possible, though, if MSS data are used to interpolate conventional soundings between survey tracklines, especially if the survey vessels obtain concurrent optical ground truth data.

If depth accuracy standards can be met, the MSS interpolation approach will be extremely cost effective. In addition, MSS imagery is shown to be a useful tool for planning and managing conventional surveys. A recommended set of procedures is outlined for incorporating MSS image data into an operational bathymetric mapping program. A comprehensive program of development and operational demonstration surveys is recommended to convincingly establish the utility and cost effectiveness of these procedures.

Approved for public release, distribution unlimited

An Assessment of the Potential Role of Multispectral Imagery in Bathymetric Charting

by

Richard T. Joy
Defense Mapping Agency Hydrographic/Topographic Center
B.S., University of Maryland, 1976

Submitted in partial fulfillment of the
requirements for the degree of

MASTER OF SCIENCE IN HYDROGRAPHIC SCIENCES

from the

NAVAL POSTGRADUATE SCHOOL
September 1984

ABSTRACT

Previous research has demonstrated the feasibility of deriving water depth information from Landsat Multispectral Scanner (MSS) digital data. However, previously published results, analysed together with two new case studies, show that the magnitude of errors (approximately 1-2 meters) in MSS single band depth estimates is too large for direct production of bathymetric charts. Better accuracy is possible, though, if MSS data are used to interpolate conventional soundings between survey tracklines, especially if the survey vessels obtain concurrent optical ground truth data. If depth accuracy standards can be met, the MSS interpolation approach will be extremely cost effective. In addition, MSS imagery is shown to be a useful tool for planning and managing conventional surveys. A recommended set of procedures is outlined for incorporating MSS image data into an operational bathymetric mapping program. A comprehensive program of development and operational demonstration surveys is recommended to convincingly establish the utility and cost effectiveness of these procedures.

TABLE OF CONTENTS

LIST OF TABLES

LIST OF FIGURES

ACKNOWLEDGEMENTS

I would like to thank my advisor, Dr. James L. Mueller, for his dedicated guidance throughout this thesis project. I especially appreciate his being available for lengthy "long-distance" consultations. I would also like to express my gratitude for the assistance I received from DMAHTC (in the form of data, references, and graphic arts support). Finally I would like to thank M. Marlow and S. Apolinario for dedicating so much of their time typing this thesis.

I. INTRODUCTION

A. BACKGROUND

The compilation of accurate and reliable nautical charts, in support of military operations and commercial shipping interests, is dependent upon the acquisition of complete and up-to-date hydrographic information. Presently, however, less than 20 percent of the world's oceans have been surveyed adequately enough to accurately portray bottom topography (Hammack, 1977). The result is that many potentially useful shipping lanes may be labelled unnavigable simply because increasingly precious ship survey time is unavailable for demarcation or confirmation of safe passage routes. More importantly, the potential for shipwrecks or groundings increases when certain shipping lanes are not routinely re-surveyed. In addition, there is increasing demand for highly accurate surveys over potential new routes.

Existing hydrographic resources are unable to respond to these requirements in a timely fashion. This situation has prompted research into alternative techniques for acquiring hydrographic information. One promising approach now being investigated is water depth estimation from multispectral satellite images measured in the visible wavelength part of the electromagnetic spectrum.

The feasibility of deriving water depths from satellite multispectral data has been demonstrated for selected areas. To obtain maximum benefits from this technique, however, further research will need to be directed towards the specific uses to which this kind of data can best be put. To explore this topic, a careful examination of an actual hydrographic charting operation was required. The Defense Mapping Agency Hydrographic/Topographic Center (DMAHTC) program was chosen as the subject of this study because of its extensive role in the global charting effort and because of its history of supporting satellite multispectral bathymetric research.

B. DEFENSE MAPPING AGENCY HYDROGRAPHIC/TOPOGRAPHIC CENTER CHARTING PROGRAM

DMAHTC is tasked with providing hydrographic and navigational information to the Armed forces of the United States, other Department of Defense components, the Merchant Marine, and mariners in general (Defense Mapping Agency Hydrographic/Topographic Center, 1980). To accomplish this mission, DMAHTC tasks the Naval Oceanographic Office (NAVOCEANO) with the ongoing acquisition of survey data. In addition, DMAHTC receives data from other countries as part of an international exchange program. Concerned mariners also supply a

significant amount of information in the form of sounding data and reports of suspected hazards.

Despite the contributions of a variety of sources, there is a significant lack of adequate hydrographic data. In particular, much of the world's coastal waters must be considered hazardous to shipping because of either inadequacy, or age, of available survey data. Figure 1 summarizes the results of a 1975 assessment of world-wide coastal hydrographic data (DMAHTC, 1984). The solid border designates those areas with no survey coverage, the diagonal hatching those with inadequate coverage, and the vertical hatching those with adequate coverage to support navigation. The study concluded that the data shortfall in coastal waters in DMA areas of responsibility would equate to over 200 years of surveying by NAVOCEANO survey ships using existing techniques.

To more effectively manage valuable survey ship time, DMAHTC is developing the Hydrographic Survey Requirements System. This computer software system is intended to allow planners to prioritize targeted areas according to the current status of the chart production program, the amount of traffic in the area, and the strategic importance of the cargo being shipped through the area.

Several potentially valuable remote sensing resources are also being developed as part of DMAHTC's Research and Development program. Candidate remote sensing systems

Figure 1. Inadequacies in World-Wide Coastal Hydrographic Data

include Synthetic Aperture Radar (SAR), blue-green LIDAR systems on low-flying aircraft, and satellite multispectral imaging systems. The last of these will be studied in detail in this thesis.

Water surface anomalies detected in SAR imagery are often associated with variation in bottom topography. This relationship may offer a useful tool for DMAHTC's hazard detection program.

Development of important fixed (conventional) wing aircraft systems is also an important effort. Laser sounding systems such as the Hydrographic Airborne Laser Sounder (HALS) can provide high density data in relatively little time (as compared to conventional launch surveys); this system has already produced sounding data within the required International Hydrographic Organization (IHO) Standards for depths to 60m. Laser technology is also being employed to calibrate passive multispectral data collected by conventional aircraft, as for example, on the Multispectral Active/Passive Scanner (MAPS). (Defense Mapping Agency Hydrographic/Topographic Center, 1984)

Ongoing research to refine algorithms for predicting depths from remotely sensed MSS images includes development of improved methods for measuring bottom reflectance and water clarity, and exploration of potential uses of multitemporal data to improve accuracy over areas with constantly shifting bottoms.

Hardcopy MSS imagery has also been used to prepare survey planning graphics in the form of zoned-depth manuscripts (Joy, 1981). These manuscripts are compiled by tracing areas of similar brightness, and give only a rough estimate of relative depth; nevertheless, the manuscripts have proven useful to planners, particularly in areas with poor chart coverage. These developments, combined with advances in satellite multispectral technology now being demonstrated by the Thematic Mapper (TM) aboard Landsat D, offer the potential for greatly increasing the effectiveness of DMAHTC's hydrographic charting program.

C. SCOPE AND FORMAT OF THESIS

This thesis will assess the potential for utilizing satellite multispectral-derived depth data in DMAHTC's hydrographic charting program. The accuracy requirements of this program are compared and contrasted to the performance capabilities of current MSS depth prediction techniques. The benefits of combining satellite multispectral data with data from other newly developed remote sensing systems is briefly discussed.

The first chapter defines the problem and presents information on DMAHTC's present and projected charting requirements and capabilities.

The second chapter contains a review of previous research in the application of multispectral data to

bathymetry, and reviews the derivation of a single band algorithm used to predict water depth from Landsat Multispectral Scanner (MSS) data. This derivation includes brief discussions of ocean optical properties and of characteristics of Landsat MSS data. Published results obtained using similar algorithms are reviewed at the end of this chapter.

Chapter III contains the results of two case studies conducted for the purposes of confirming previously published results and of assessing the accuracy of MSS derived depths under conditions approximating normal operating procedures. Included are descriptions of the data sets and a discussion of the processing techniques.

The analysis of results and conclusions are presented in Chapter IV. The impact of error levels on the potential use of MSS derived depths is the principal concern of this discussion.

Based upon the conclusions drawn in Chapter IV, several recommendations are presented in Chapter V. These include both short-term implementation recommendations and long-term research goals.

Appendix A contains a discussion of the Landsat series of satellites, with emphasis on the MSS data characteristics. Appendix B contains a description of the image navigation procedures used in the case studies described in this thesis.

II. WATER DEPTH ESTIMATION FROM MULTISPECTRAL SATELLITE IMAGERY

The estimation of water depths from measurements of upwelled radiance is simple in concept. In areas where the water is clear and spatially homogeneous, and where the sea floor is composed of light colored material of high reflectivity (compared to that of water), reflected radiance at the sea surface will increase systematically as water depth decreases. If both the optical properties of the water and the reflectance of the bottom are spatially homogeneous, then this relationship may be exploited in a quantitative way to estimate water depth from remotely sensed images of upwelled radiance. When this technique is applied, using measurements from satellites above the earth's atmosphere, it is also necessary to take into account the radiance contributions and attenuation associated with the earth's atmosphere.

Previous work has demonstrated at least the conceptual feasibility of this technique using Landsat MSS images of shallow water sites which were known to be characterized by exceptionally clear water and bright sandy bottoms. These results will be reviewed in this chapter, and subsequently compared with results of two case studies analyzed as part of this thesis project. The purpose of this analysis is to assess the potential feasibility of applying this

technique, in a useful and cost-effective way, within DMA's operational bathymetric survey program. Consideration will be given to possible uses of MSS derived water depth maps as planning tools, quality control information, and as interpolation fields (between survey ship tracklines), as well as to direct use in bathymetric mapping. In each case, feasibility and utility are determined primarily by the errors which must be attributed to the MSS derived depth estimates.

A. THE LANDSAT MULTISPECTRAL SCANNER (MSS)

The MSS is an imaging radiometer flown as one of the principal instruments on the Landsat series of earth observation satellites. Each Landsat satellite is operated in a sun synchronous orbit at approximately 900 kilometers (km) altitude, with its ascending node occurring near 1030 local apparent time. The satellite sub-orbital track re-visits a particular geographic location, and allows MSS image coverage (clouds permitting) once every 18 days; although this sampling interval makes the Landsat MSS poorly suited for most oceanographic applications, it is well-matched with the time scales of changes in bathymetric features. (Storms may rework shoals extensively within a few days, but the changes may be readily assessed by Landsat image composites assembled over a period of several weeks, or months).

The MSS images earth/atmosphere radiance patterns by scanning a mirror over an 11.6 degree arc centered at nadir and perpendicular to the orbital track. Upwelled radiance is focused by the scan mirror through a telescope and optics train into a spectrometer. Within the spectrometer, the angular field of view of the telescope is divided into six segment beams in the along-track direction; each of these along-track segment beams is then directed to one of six individual detectors in each of four wavelength bands. During each cross-track scan of the mirror (repeated every 33 milliseconds) all 24 detectors are sampled every 9.95 microseconds to yield, for each of the four channels, six adjacent cross-track lines of digital radiance values at each of 3240 picture elements (pixels). A single Landsat MSS image combines 360 successive six-line scans to form a 2340 X 3240 pixel array, with each pixel's value in each channel representing radiance associated with a 79m X 79m area at the earth's surface.

The MSS channels (bands), applicable to this study, designated four through six, each measure radiance in a 0.1 micrometer (μm) wavelength interval centered at 0.55, 0.65, and 0.75μm respectively; the MSS Band 7 spans a 0.4 μm interval centered at 0.95μm. Of these, the wavelength interval of MSS Band 4 spans the region of minimum absorption by water, which makes it the most useful channel for single-channel water depth estimation. Band 5

spans a region where absorption by water limits the effective penetration depth to approximately 3m; it has been used, together with Band 4, in a two-channel water depth algorithm applicable to extremely shoal areas (Polcyn, et al., 1977). In the wavelengths associated with Bands 6 and 7, effective optical depths are limited by strong absorption to the top few centimeters (cm) of the water column. (Unfortunately too, the wavelength intervals associated with these channels are too broad to use them in atmospheric correction algorithms of the type developed for the Nimbus-7 Coastal Zone Color Scanner (CZCS)) (Gordon, et al., 1983).

The characteristics of the MSS and of its digital data are reviewed more completely in Appendix A, and in yet more detail in the report by Taranik (1978).

B. ALGORITHM FOR CONVERTING MSS RADIANCES TO WATER DEPTHS

The total aperture radiance L_{t4} measured by the MSS in Band 4 may be approximated by the equation

$$L_{t4} = L_r4 + L_{a4} + \frac{E_4t_4}{Q} R_4 - \frac{E_4t_4}{Q} R_4e^{-2K_4D} + \frac{E_4t_4}{Q}R_{b4}e^{-2K_4D}, \quad (1)$$

where total radiance L_{t4} is calculated from the Band 4 digital counts as (Appendix A and Warne, 1978)

$$L_{t4} = 8.3\ DN/128, \quad (2)$$

L_{r4} is Rayleigh path radiance due to backscatter by atmospheric gas molecules,

L_{a4} is atmospheric path radiance due to backscatter by aerosols,

E_4 is incident solar irradiance just below the sea surface (E_4 is estimated from solar irradiance at the top of the atmosphere, with adjustment for time of year, single scattering Rayleigh plus ozone attenuation through the atmosphere, and Fresnel transmittance through the sea surface. Values used are based on the similar CZCS algorithms as contained in Gordon, et al., (1983),

R_4 is the irradiance reflectance of a water column of effectively infinite optical depth measured just beneath the sea surface,

Q is the ratio of upwelled radiance to incident irradiance just below the sea surface, and following Austin (1974) it is assumed that Q = 5 (if the surface just beneath the air-sea interface were Lambertian, then Q would equal π),

t_4 is the diffuse transmittance of the atmosphere and ocean, which following Gordon, et al. (1983) is approximated as:

$$t_4 = \frac{1 - \rho(\theta)}{m^2} \; e^{-\tau_{R_4}/2 + \tau_{O_{34}}/\cos\theta} \qquad (3)$$

where τ_{R4} and $\tau_{O_3 4}$ are Rayleigh and ozone optical depths respectively (with values interpolated from those in the same reference), m is the refractive index of water (assumed m = 1.33), and $\rho(\theta)$ is the Fresnel reflectance of the air sea interface at angle θ,

R_{b4} is the reflectance of the ocean bottom, which is assumed to be Lambertian,

K_4 is the vector irradiance attenuation coefficient (sometimes called the "diffuse attenuation coefficient" of the water column in m^{-1}, and

D is water depth in m.

The units of all radiance terms are mW cm^{-2} sr^{-1} μm^{-1}, and those of irradiance are mW cm^{-2} μm^{-1}. The subscript "4" denotes that the value applies to the effective monochromatic wavelength to be associated with Band 4, which is assumed to be 0.55 μm.

Using approximations developed for the CZCS (Gordon, et al., 1983), the Rayleigh and aerosol path radiance terms vary to first order as $\sec\theta$, where θ is the viewing zenith angle. Over an entire Landsat image, the 5.8 degree variation about nadir in viewing angle introduces less than 0.5 percent variation in these path radiance terms and they may be treated as constant for the scene. If it is also assumed that the optical properties of the water (K_4 and R_4) are constant over the entire ocean area covered by an

image, then for any deep water pixel (i.e. D is greater than $3K_4^{-1}$) the radiance L_{t4} may be expressed as,

$$L_{\infty 4} = L_{r_4} + L_{a_4} + \frac{E_4 t_4}{Q} R_4, \qquad (4)$$

which may thus be assumed to be constant over the entire image. A measured value of $L_{\infty 4}$, obtained by averaging over deep water pixels in a given Landsat image, may then be substituted for the first three terms on the right-hand-side (rhs) of (1). The fourth term on the rhs of (1) represents the radiance reflectance at depth D from an optically infinite water column below that depth, assuming ocean optical properties to be homogeneous vertically, as well as horizontally. The first four terms on the rhs of (1) are thus seen to represent the sum of path radiances from the atmosphere and water column of depth D above the sea floor. The last term accounts for radiance reflected from the sea floor itself.

Substituting (4) into (1), and assuming bottom reflectance R_{b4} to also be constant over the imaged area, the resulting equation may be solved for water depth D as

$$D = \frac{1}{2K_4} \ln (R_{b4} - R_4) - 1/2k_4 \ln\left[\frac{(L_4 - L_{\infty 4})Q}{E_4 t_4}\right] \qquad (5)$$

With the above assumptions for a particular site and image, Equation (5) is of the form:

$$D = A + BX \tag{6}$$

where the variable

$$X = \ln \frac{(L_4 - L_{\infty 4})Q}{E_4 t_4} \tag{7}$$

and the coefficients A and B are related to ocean and bottom optical properties by the equations

$$A = \frac{1}{2K_4} \ln (R_{b4} - R_4) \tag{8}$$

$$B = \frac{-1}{2K_4} \tag{9}$$

In use, the coefficients A and B are determined by least squares regression for a sample of radiances extracted from each image at control positions where depths D are known from contemporaneous in situ measurements. Then, equations (8) and (9) are used to calculate the values of K_4 and $(R_{b4} - R_4)$ to be associated with that image.

The principal sources of error in the above algorithm arise from spatial variabilities in atmospheric aerosols, ocean optical properties, and bottom reflectance.

Research with the CZCS has demonstrated that aerosol radiance values, typically vary on scales as small at 10km with amplitudes comparable to those of water radiance, so that pixel-by-pixel atmospheric correction algorithms must be used (Gordon, et al., 1983). As mentioned in the previous section, however, the characteristics of the Landsat MSS Bands 6 and 7 are not well suited for this correction, and it is necessary to neglect aersol radiance variations by assumption. As a minimum precautionary measure, however, enhanced versions of the Band 6 and 7 images should be inspected for evidence of organized patterns of brightness attributable to variations in aersol density (including smoke plumes and/or brightness patterns which appear to be spatially related to cloud patterns); the Band 4 data should be discarded for areas where such patterns exist.

Variations in ocean optical properties can arise from spatial variability in concentrations of marine phytoplankton, inorganic particulates, and/or dissolved organic compounds ("gelbestoffe") (Jerlov, 1976). In general, the MSS water depth estimation may only be applied in relatively clear-water environments which are not fed by a significant flux of terriginous material due to coastal

runoff or estuarine discharge. Therefore, waters in which the optical properties are significantly influenced by inorganic particles, the primary source of which is terriginous runoff, are not candidates for this depth estimation technique. Highly productive oceanic regions are similarly excluded, simply because the concentrations of phytoplankton in productive coastal waters reduce the optical depth to a small fraction of water depth and bottom reflections are not seen. (However, some sites may be productive in some seasons, but relatively barren in others, so that in certain months water clarity may permit estimation of bathymetry from MSS images). Since the major sources of dissolved organic compounds in the ocean are humic compounds contributed by terrestrial runoff and decayed phytoplankton materials in highly productive waters, variability of "gelbestoffe" concentration would be a factor only in situations which would be otherwise excluded from consideration here on the basis of more easily detected contributors to ocean optical properties.

The reflectance of the sea bed is dependent upon the composition, roughness, and to some extent, upon the slope of the bottom. Of these three characteristics, a change in composition (which here refers to both lithographic and vegetative characteristics) is the most significant factor in estimating bathymetry from reflected radiance. The water depth algorithms under consideration attribute change

in signal value to variation in the depth of a bottom of constant reflectance. However, if the bottom reflectance was assumed to be that of a very bright, sandy bottom, and a pixel was observed an area of dense bottom vegetation, the predicted depth would be much greater than the actual depth. The reverse case is also possible, although conservative depth estimates are preferable as they pose no actual danger to ships. Errors in depth estimation resulting from assuming a constant seabed composition are possible at all depths which can be sensed and require a conservative estimate of R_{b4} to bias errors towards underestimates. This "safe bias" procedure will be discussed in conjunction with error analyses in Chapter II, IV, and V.

The effect of texture changes, independent of composition variation, should be significant only in shallow waters (with depths less than 5m). This is because texture variation affects reflection of direct radiation, and downwelling light becomes increasingly diffuse with depth. The effects of texture changes upon reflected radiance are further reduced since the seabed itself acts as a diffuse reflector. For these reasons, the effect of slope changes should also be significant only in shallow waters with steep banks (Warne, 1978).

The residual standard deviation of the regression analysis of the control sample used to determine

coefficients A and B provides a crude measure of the combined effects of spatial variability of bottom reflectance and water optical properties. In situ optical observations, made in conjunction with measurement of water depths at control positions, can (at least in principal) be used to separate these contributions. It is particularly important to detect the presence of patchy variations in phytoplankton concentrations and/or bottom vegetation, since either occurrence can lead to potentially serious overestimates of water depth. Techniques for routinely measuring optical properties during in situ bathymetric surveys are briefly discussed in Chapter V.

Equation (1) neglects reflected skylight, and assumes that sun glitter is negligible. Since this water depth algorithm is based on relative variations in upwelled radiance over a region spanning both deep (optically infinite) and shallow water, and since it is reasonable to assume that skylight is constant over a nearly cloud-free Landsat image, the neglect of reflected skylight will, at worst, introduce a bias error which will be absorbed in the model's empirical B coefficient (Equation 5). Errors due to neglect of sun glitter can be more serious at low latitudes in summer months. With solar zenith angles less than 30 degrees, sun glitter can be significant even for near nadir viewing angles (Cox and Munk, 1954); this error source can be especially serious in areas where small scale

variations in surface winds (e.g., near coasts and islands) introduce variations in glitter radiance. Therefore, this algorithm should be used with extreme caution if applied to an image associated with a solar elevation much in excess of 55 degrees.

C. PREVIOUS RESULTS

In the late 1960's Brown et al. (1971) began developing techniques for using passive multispectral scanner data for bathymetry. By 1973, the basic principles of deriving depths from single band data had been demonstrated using both aircraft and MSS data (Brown, et al., 1971). Development efforts were then extended to two-channel techniques which were designed to reduce the sensitivity of the water depth algorithm to variability in bottom reflectance and optical properties of the water column. In tests conducted over the Little Bahama Bank, with low gain Landsat MSS data, single-band techniques were used to predict depths to 9m, and the dual-band method was used to predict depths to 3m (Polcyn and Lyzenga, 1975).

In 1975, the National Aeronautics and Space Administration (NASA) and the Cousteau Society jointly sponsored an ocean bathymetry experiment designed to determine 1) the maximum depth measurable using high gain MSS data from Landsat 1 and 2, and 2) the potential accuracy improvement of the MSS depth estimates when

supported by in situ measurements of relevant ocean optical properties. Tests were conducted in two areas of different optical properties. The first area was located on the northern edge of the Great Bahama Bank, west of the Berry Islands. This area was chosen for its relatively high bottom reflectance (determined to be 26 percent), and water clarity (K_4=0.058m^{-1}). The second area was located off the east coast of Florida, near Hollywood. For this area, the bottom reflectance and irradiance attenuation coefficient, K_4, were determined to be 20 percent and 0.11m^{-1} respectively. The accuracy of the MSS derived depths was determined through comparisons with fathometer readings taken at the time of satellite imaging (Polcyn, 1976).

At the Berry Islands Test Area, MSS depth measurements were determined to depths as great as 22m with an rms error of 10 percent, and bottom reflected radiance patterns were detected in the MSS images from depths as great as 40 meters. During this study, depth maps were prepared from the Landsat-derived data for that portion of the Berry Island Test Area covered by N.O. Chart 26320. Several different processing techniques were tested in the preparation of the depth maps, including smoothing to reduce the effects of varying responses among each of the satellite's six sensors, and in turn, enhancements to reduce the coarsening effect of smoothing (Polycyn, 1976).

In 1977, Hasell reported on the development of the M8 active/passive scanner system. This system combined a multispectral scanner with a pulsed laser system (Hasell, 1977) and was designed to be carried aboard conventional aircraft. The bathymetric applications of the M8 system were tested over several sites in the Bahamas in August 1978, under a contract with DMA. The depth data from the active laser system was used as ground truth to compute a relationship between bottom depth and passive scanner signal value. This formulation was then used to predict depths, given only scanner values. For the North Cat Cay test site , depths under 15m were predicted with an rms error of 0.72m, and for the Bimini test site, with an rms of 0.923m (Lyzenga, 1981).

The potential usefulness of depth maps prepared from high gain MSS data in pre-survey reconnaissance work was demonstrated by the Environmental Research Institute of Michigan (ERIM), in 1977 under a contract to DMA (Polcyn, et al., 1977). Seven depth-zone maps were produced for portions of the Little and Great Bahama Banks, using water depth algorithms developed previously. The maps were then compared with the existing chart coverage, and the satellite maps revealed several areas requiring re-surveying.

An independent study by Warne (1978) addressed practical applications of Landsat imagery to hydrographic mapping,

with specific emphasis on applications of the technique in waters near Australia. Warne developed an interactive computer software system called Hydrographic Mapping System (HYDMAP), which allows an interpreter to interactively segment an MSS image into areas of consistent optical characteristics. Using HYDMAP, and applying additional radiometric corrections to each Landsat image, Warne prepared zoned depth maps for two test areas in the waters between Cape York, Australia, and Papua, New Guinea. The depth prediction techniques used were found to be accurate to within 1m rms to a depth of 16m.

Research on this topic meanwhile continued in the United States. To further evaluate the accuracy of single-channel depth prediction techniques, Lyzenga and Polcyn (1979) compared depths derived from Landsat MSS to leadline and fathometer sounding data at 10 stations in the Bahamas Photobathymetric Calibration Area. The water attenuation coefficient used was the same as that measured for the Great Isaac station during the NASA/Cousteau Photobathymetric Survey Study of 1975-1976 (Lyzenga and Polcyn, 1979). Bottom depths were predicted using two sets of bottom reflectance values. The first set of calculations used the value of 0.22; this value had been used previously in processing the same scene. A second set of calculations were based upon bottom reflectance values for each station which were derived from underwater

photographs of the bottom and test panels of known reflectance (Lyzenga and Polcyn, 1979).

Tables 1 and 2 present the results obtained using each set of bottom reflectance values. The following information is presented for each station: measured depth, MSS-derived depth (predicted depth), the bottom reflectance value used to predict depth (R_{b4}), and the difference between measured and predicted depth. The standard error of prediction was 2.6m using the assumed value R_{b4}=0.22 and 1.9m using individually measured values of R_{b4}.

TABLE 1
ERIM Study-Results Using Single Bottom Reflectance Value

Station	Measured Depth (D_m)	Predicted Depth (Dp)	D_m-Dp*	R_{b4}
C-5	9.8m	7.7m	+2.1	0.22
D-7	9.1m	9.1m	0.0	0.22
F-11	9.8m	11.5m	-1.7	0.22
G-12	10.4m	11.5m	-1.1	0.22
H-13	4.9m	3.3m	+1.6	0.22
I-14	6.7m	8.3m	-1.6	0.22
J-16	12.5m	16.5m	-4.0	0.22
A-17	6.1m	6.7m	-0.6	0.22
B-18	10.7m	15.3m	-4.6	0.22
D-21	6.1m	9.1m	-3.0	0.22

Standard Error of Prediction 2.6m*
Mean Bias = -1.29*
Source of Tables: (Lyzenga and Polycn, 1979)
*Derived Values

TABLE 2

ERIM Study-Results Using Individual Bottom Reflectance Values

Station	Measured Depth (D_m)	Predicted Depth (Dp)	D_m-Dp*	R_{b4}
C-5	9.8m	7.1m	+2.7	0.20
D-7	9.1m	9.7m	-0.7	0.24
F-11	9.8m	11.8m	-2.0	0.23
G-12	10.4m	10.5m	-0.1	0.19
H-13	4.9m	3.9m	+1.0	0.24
I-14	6.7m	3.0m	+3.7	0.10
J-16	12.5m	11.2m	+1.2	0.10
A-17	6.1m	7.0m	-0.9	0.23
B-18	10.7m	12.7m	-2.0	0.15
D-21	6.1m	7.0m	-0.9	0-16

Standard Error of Prediction 1.9m*
Mean Bias = +0.2*

Source of Tables: (Lyzenga and Polycn, 1979)
*Derived Values

Assuming constant water clarity from site to site, as Lyzenga does in this investigation, the relationship between measured depth and predicted depth reveals the effect of varying the bottom reflectance value. The assumed constant value of 0.22 yielded deeper depths than were actually measured at all but three stations; this is reflected in the negative value (-1.29m) of the mean bias. This result indicates that the true bottom reflectance at the majority of the stations was less than 0.22., an inference confirmed by inspection of actual reflectances in Table 2. When the lower, measured bottom reflectance values were used at those stations with negative residuals (G-12, B-18, and D-21, for example) predicted depths were much closer to the measured depths (Table 2). Similarly,

for those stations at which the inferred value gave depths which were too shallow (C-5 and H-13 in Table 1), the higher measured values yielded better results (Table 2). Accordingly, the standard error of prediction improved (from 2.6m to 1.9m). The mean bias also became significantly smaller and shifted to a positive value, indicating more conservative predictions. When the measured bottom reflectance value was greater than 0.22, for those stations at which the inferred depth values were too deep, the result was even greater residuals, as shown by stations F-11 and A-17. Similar reasoning can be used to explain the results obtained at each of the other stations.

The tendency, noted above, for estimated depths to be dangerously biased towards overestimates, points to the need to independently estimate the spatial variabilities in ocean optical properties and bottom reflectance using concurrent ground truth data. Further, it will be desireable to use some minimum probable value for bottom reflectance R_{b4}; this procedure will bias MSS depth values towards underestimates, and reduce the probability of depth overestimates greater than some critical value (e.g. 0.3m) to a level to be determined by future research. This "safe bias" concept is discussed in more detail in Chapters IV and V.

For five stations there was a loss of accuracy using the measured values; the measurement of bottom reflectance was unsatisfactory. Lyzenga, in fact, proposes that the bottom photographs used to measure bottom reflectance may have favored the bottom vegetation more than the sand, and/or that they reduced the contrast between very dark and very bright areas (Lyzenga and Polcyn., 1979). In either case, the bottom reflectance was the average value for the instantaneous field of view of the Landsat sensor.

A second possible explanation for the reduced accuracy at these five stations is that the initial assumption of constant water clarity was incorrect. Lyzenga states that conditions were unsuitable for obtaining in situ measurements during the time of the experiment, so that no comparison set was available. However, this issue is discussed further in section III.E, where Lyzenga and Polcyn's results will be compared with those obtained for the same Landsat scene in the present investigation. These two experiments will then form the basis for the discussion of error impact analysis and potential uses for satellite multispectral imagery in bathymetric mapping (Chapters IV and V).

D. SYNOPSIS

The principles of producing water depth from single-band MSS data are sufficiently understood to begin to assess the

potential role of this tool in bathymetric survey operations. Research has shown that the usefulness of these procedures is limited to clear, homogeneous waters with bright bottoms, precluding their use in areas of high organic productivity or in coastal waters receiving significant terrigenous runoff. Likewise, the principal error contributors have been identified as variability in atmospheric aerosols, ocean optical properties, and bottom reflectance. Research efforts have also resulted in the preparation of potentially useful prototype products.

The first step in defining the usefulness of MSS-derived bathymetric products is to quantify expected error levels associated with the predicted depths. Two case studies (designed to simulate operational procedures) will be used, in conjunction with those results reported by Lyzenga and Polcyn (1979), to derive values for expected error levels. These values will then be used to assess the cost benefits of combining multispectral data with control tracklines to obtain nearshore hydrographic data.

III. SELECTED CASE STUDIES

A. INTRODUCTION

The previous experiments reviewed in Chapter II have indicated the potential usefulness of Landsat MSS-derived depths to the hydrographic community. To more clearly define the potential role of this tool, two case studies were conducted. The studies were designed to reexamine published results under conditions approximating operational procedures, and to assess the applicability of these procedures under various ocean optical conditions. Much of the discussion in Chapter IV, on the impact of error sources, and on the cost benefit aspects of this use of Landsat MSS data, is drawn from the results of this investigation.

B. SITE CHARACTERISTICS

Several geographic areas were initially identified as being suitable for this investigation. These were selected for their relatively high, and reasonably homogenous, bottom reflectances, and for their variety in water clarity. Final site selection was based upon the availability of both high-gain Landsat tapes and contemporaneous survey data. Four sites were chosen from two test areas satisfying the selection criteria.

Test Area 1 is located on the northwest-western margin of the Great Bahama Bank. Two sites were selected from this test area. Site 1 is located in the waters south and west of the island chain formed by South Cat Cay, North Cat Cay, and Gun Cay (Figure 2). The site measures approximately 5.5 nautical miles southeast to northwest and approximately 1.75 nautical miles northeast to southwest. Site 2 is approximately 15 nautical miles from Site 1, located off the northwest coastline of North Bimini (Figure 3). This site measures nearly 4.5 nautical miles north to south and averages 2 nautical miles, on the average, east to west. These correspond to portions of areas 1 and 3, respectively, of the Bahama Photobathymetric Calibration Survey of 1980.

Test area 2 is located on the west Florida shelf between 28° 10' N and 27° 30'N. As with the Bahamas Test Area, data was collected from two sites within Test Area 2; these are labelled Site 3 and Site 4 (Figure 4). The location and seaward extent of these sites was fixed by the boundaries of the survey from which the set of control depths were taken. Site 3 extends approximately 15 nautical miles off the Florida coast at Tarpon Springs and measures almost 6 nautical miles north to south. The orientation and evenness of the depth contours in Figure 4 reflect the steady increase of depth with seaward distance. For this reason data spanning a suitable range of depths was

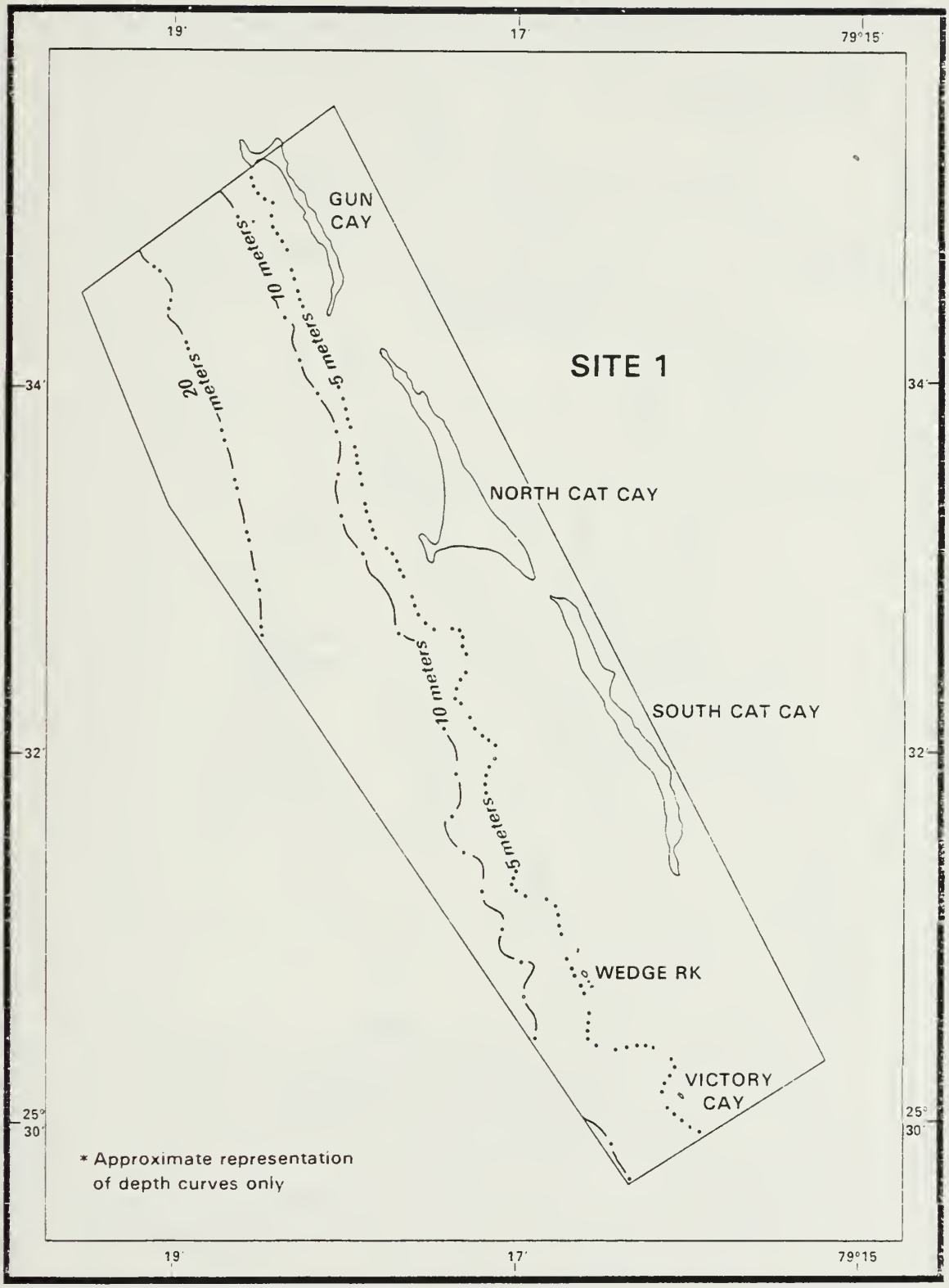

Figure 2. Case Study 1 - Site 1

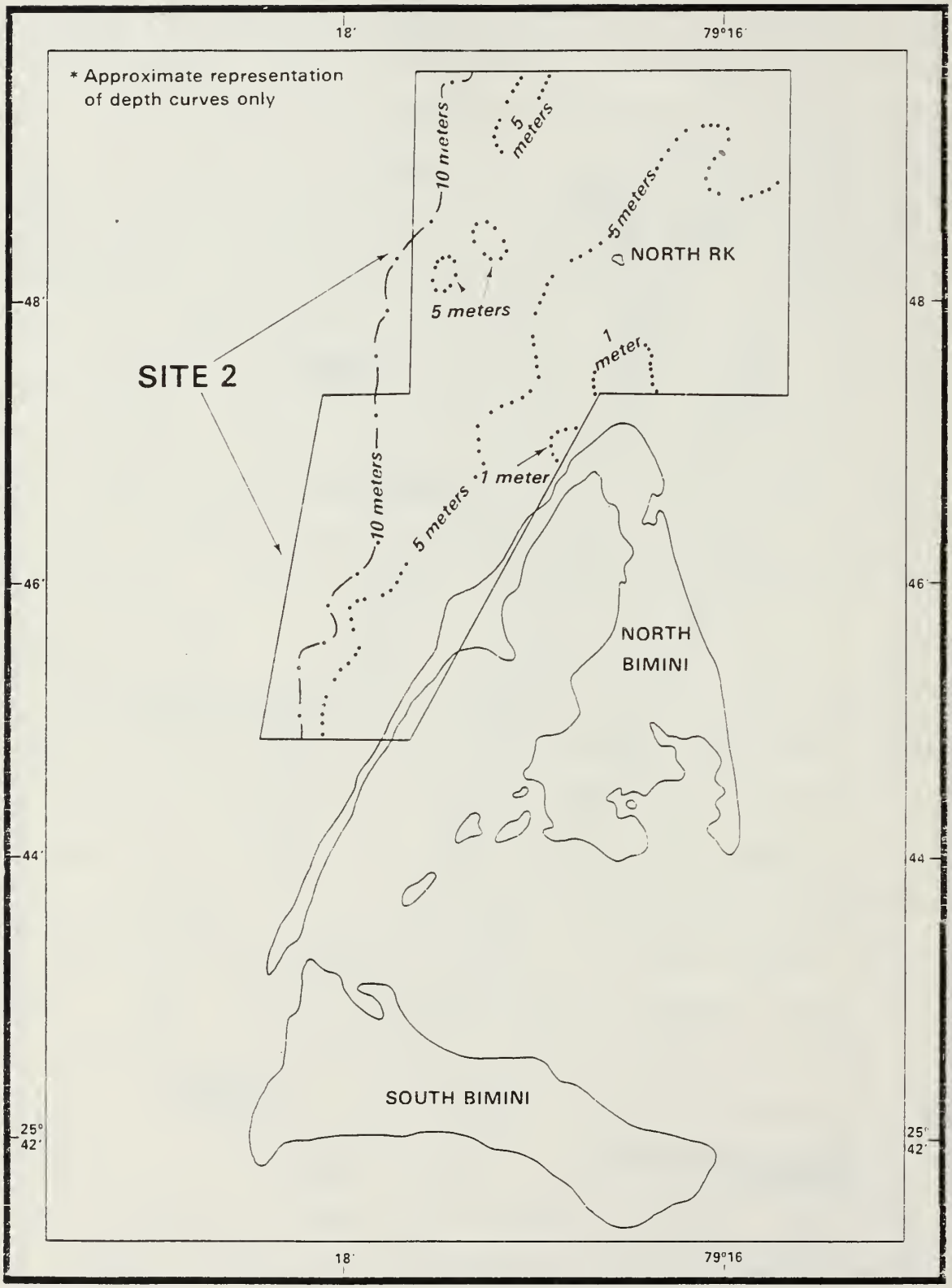

Figure 3. Case Study 1 - Site 2

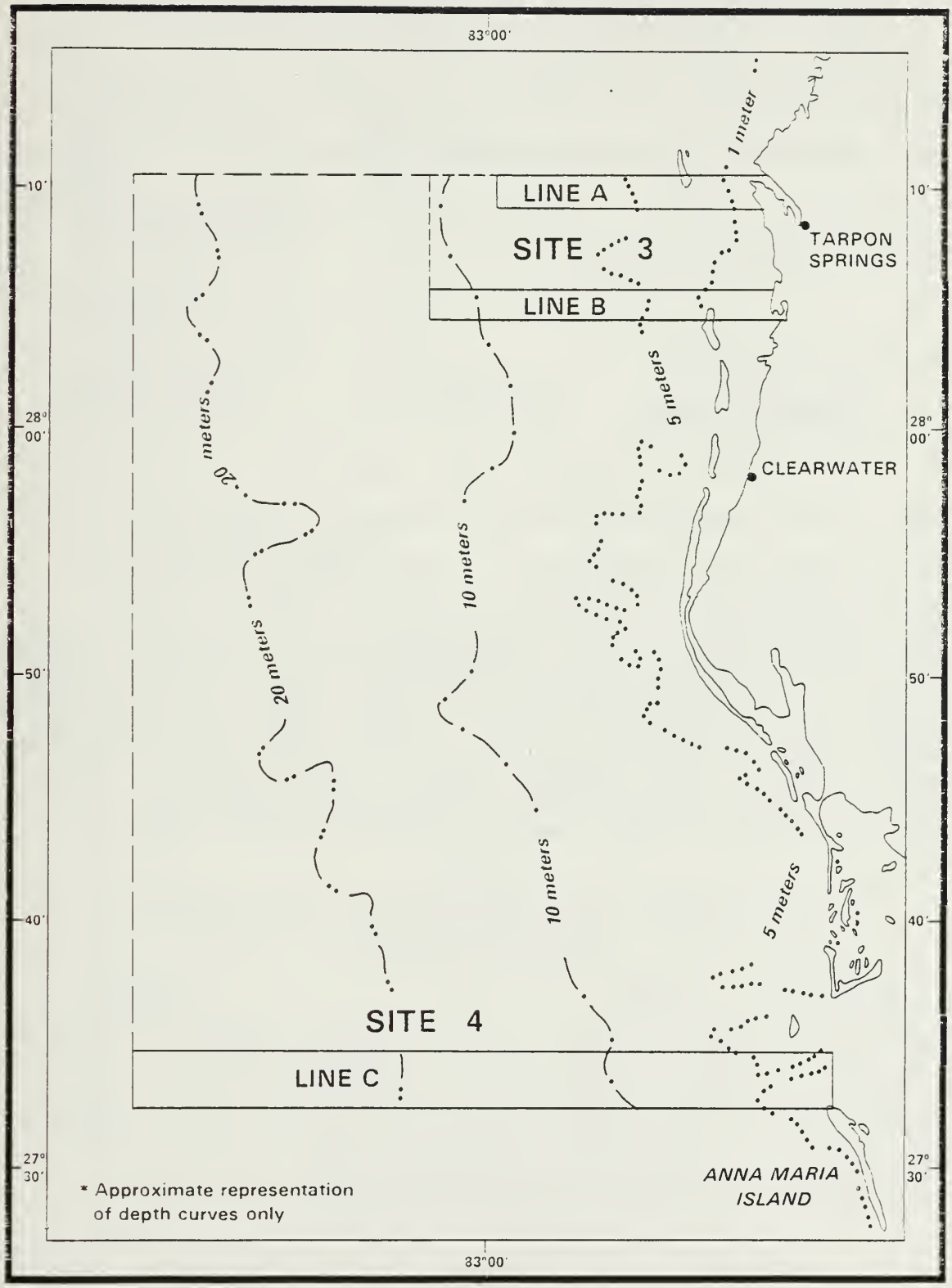

Figure 4. Case Study 2 - Sites 3 and 4

extracted by sampling along transects perpendicular to the shoreline; in Site 3, these are labelled Lines A and B.

Site 4 is located approximately 35 nautical miles south of Site 3, and extends almost 30 nautical miles offshore. The difference in seaward extent between Sites 3 and 4 reflects the requirements of the original survey from which control depths were drawn.

C. DATA DESCRIPTION

1. Landsat Images

The Landsat images used in this investigation received the standard NASA bulk processing applied to all pre-1978 MSS data (Appendix A). The data was released in a "band-interleaved by pixel-pair format" (ERTS-format), on 9-track, 1600 bpi computer compatible tapes (CCTs). The two MSS images analysed in this project were obtained from DMAHTC, NASA, and Goddard Space Flight Center. The characteristics of each image are summarized in Table 3.

TABLE 3
Identification of Landsat-1 MSS Imagery and Key Radiation Parameters for Case Study Areas 1 and 2

Test Area	1(Great Bahamas)	2(West Florida Shelf)
Recording Mode	High Gain	High Gain
Date	24 December 1975	13 March 1976
Time	1443Z	1435Z
Solar Elevation	28	48
Incident Solar Irradiance (E_4) ($mWcm^{-2}\ m^{-1}$)	85.759	139.55
Deep Water Radiance (L_4) ($mWcm^{-2}sr^{-1}\ m^{-1}$)	2.853	4.766
Cloud Cover	less than 10%	less than 10%
Scene Number	5249-1443500	85360-1453500

2. Water Depth Data

Water depths used to estimate the precision of depths calculated using Equation (2)-(5) and Landsat MSS radiances were taken from recent NOS hydrographic survey sheets and from NOS charts. In the Florida Test Area, both sources of comparative depth data were used (Table 4).

TABLE 4
Sources Used for Control Depths: West Florida Shelf Test Area

Source			Date	Scale
NOS Survey Sheet	H-9509		4/75 - 8/75	1:20,000
	H-9510		4/75 - 8/75	1:20,000
	H-9338		4/75 - 8/75	1:20,000
NOS Chart	1140	19th Ed.	8/15/81	1:40,000
	11412	25th Ed.	5/17/80	1:80,000
	11414	27th Ed.	3/27/82	1:40,000
	11424	13th Ed.	4/25/81	1:80,000

Since the survey data are more accurate, the NOS charts were used only where the survey data did not adequately cover the Test Area and in cases where densely clustered charted depths showed no depth variation over the sampling area. All depth data used in the Great Bahama Bank Test Area was extracted from survey data collected by the R/V Adam's Folly in 1980, in conjunction with the Bahamas Photobathymetry Study being conducted by DMAHTC. This Test Area has been frequently surveyed and the data showed no significant variations in bottom topography over the period 1976-1980 (James Hammack, DMAHTC, Personal Communication, 1981). The control depths over the West Florida Shelf were taken primarily from survey data collected less than one year earlier than the corresponding Landsat image. Since there were no effects from major storms in the intervening months, it is assumed that the Landsat images and the comparison depth samples are effectively contemporaneous.

D. METHODS OF ANALYSIS

The relationships between water depth, D, and Landsat counts are expressed in Equations (4), (5), and (6). For each test area, samples were prepared in which computed values of the log reflectance anomaly, X, as defined in (7), were paired with survey depths.

A navigation algorithm was developed to identify the pixels corresponding to the geographic position of each

sample depth. The procedure was tested using landmarks identifiable on the Landsat scenes, yielding a circular error (at the 90 percent confidence level) of 113.3m for the Great Bahama Bank scene, and 143.5m for the West Florida Shelf scene (Appendix B).

In all cases, both X and D values represent the average over a ground area roughly equivalent to the appropriate navigational circular error. Therefore, each MSS4 sample value represents the average of a 3x3 pixel matrix for the Bahamas scene, and of a 4x4 pixel matrix for the Florida scene.

The average control depth values used in the Bahamas test area were computed by first plotting track lines and speeds of the survey vessel from the positional and timing information on the data tape, and then determining the number of sounding events covering an area 216m square (equivalent to the navigational circular error). Because ship speed varied from track line to track line, and because the density of track lines also varied, these computations were made separately for each track line used.

Average depth values from the West Florida Shelf Test Area were computed by averaging each plotted depth (from either a sounding sheet or a chart) within the area equivalent to a 187m square area (corresponding to the circular error).

Survey depth values for each test area were corrected to match the tidal stage at the time of Landsat MSS observation. Following Polcyn et al. (1977), a correction factor of +0.61m was applied to all Bahamas depths. Tidal corrections for the West Florida Shelf depths were computed from data supplied by the Tides Branch of the National Ocean Survey (NOS), Rockville, Maryland. Predicted tidal height for Site 3 at the time of the Landsat observation was calculated to be 0.55m above Mean Low Water (MLW) (predicted form the Clearwater Tidal Station); predicted tidal height for Site 4 was calculated to be 0.13m above MLW (predicted from the St. Petersburg Tidal Station). As with the Great Bahama Bank data set, all West Florida Shelf tidal corrections were applied to the surveyed depths, to bring these into agreement with the Landsat-derived depths.

For each sample, a scatter plot of X versus D was prepared and inspected for possible outliers. Each suspected outlier was tested using the statistic and Table of Percentage Points for the Studentized Maximum Absolute Deviate prepared by Halperin (1955). Each data point which failed the initial outlier test was re-evaluated by comparing it's MSS4 and depth sampling statistics to those computed for the entire sample set. If the local variance of the outlier cell was less than the average local variance for the overall data set, the point was discarded. On the other hand, if the local variance for either depth

or MSS4 count exceeded the average of the entire sample set, local outliers were discarded and a new depth and/or count average was computed. A new outlier test was then performed with the revised values, and any points again failing the test were discarded.

The sample for each test site was divided into a control sample and a test sample. For each site (excluding Site 2, which had too few points) a simple linear regression was performed to compute the coefficients A and B of Equation (5), using data from the test sample. From the values of A and B, local values for K_4 and R_{b4} were calculated from Equations (8) and (9). These values were compared, for plausibility, to published representative values for the region (Jerlov, 1976). Equation (5) was then used to compute corresponding depths D for each X (Equation (7)) value in the control sample.

An additional linear regression analysis was performed for each of the two test areas using the combined test samples from each of the two included sites. The predicted depths obtained from this set of coefficients were compared to the former set to assess the regional dependence of the technique.

E. RESULTS

The points selected for each test sample are depicted graphically in the scatter plots of Figures 5-8; the

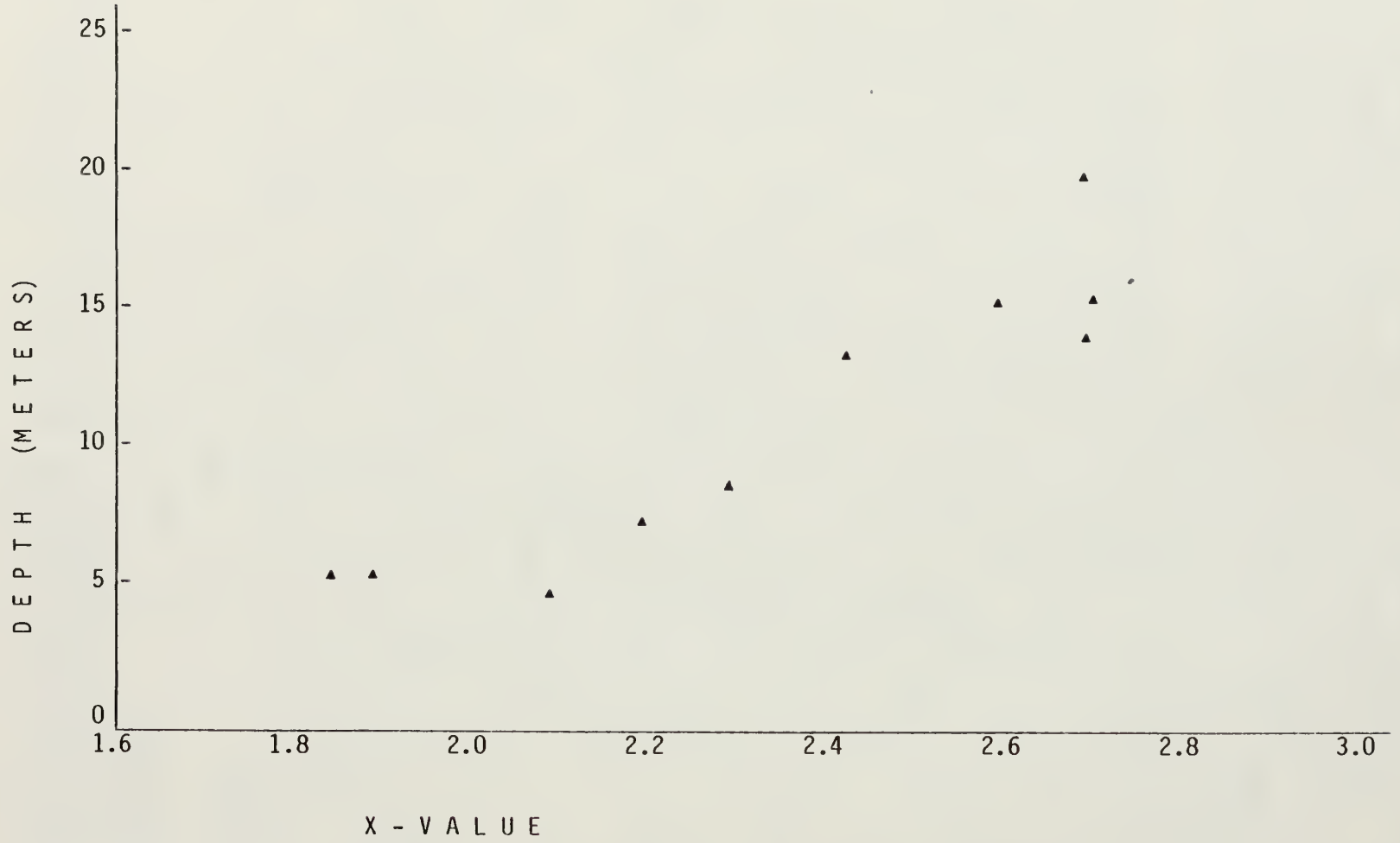

Figure 5. Plot of Log Reflectance Anomaly (X) vs. D for Site 1 Test Sample

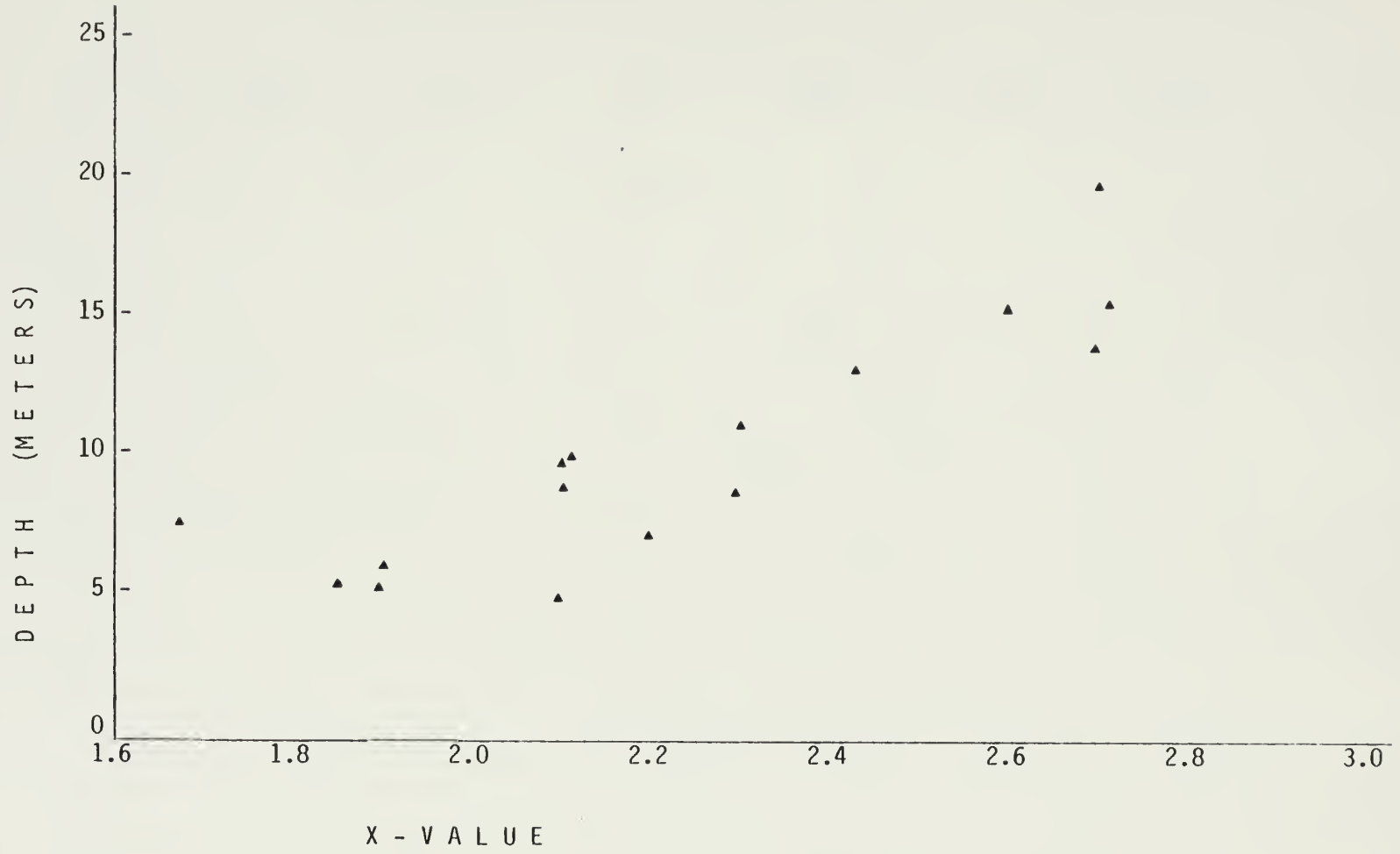

Figure 6. Plot of Log Reflectance Anomaly (X) vs. D for Site 1 and Site 2 Combined Test Sample

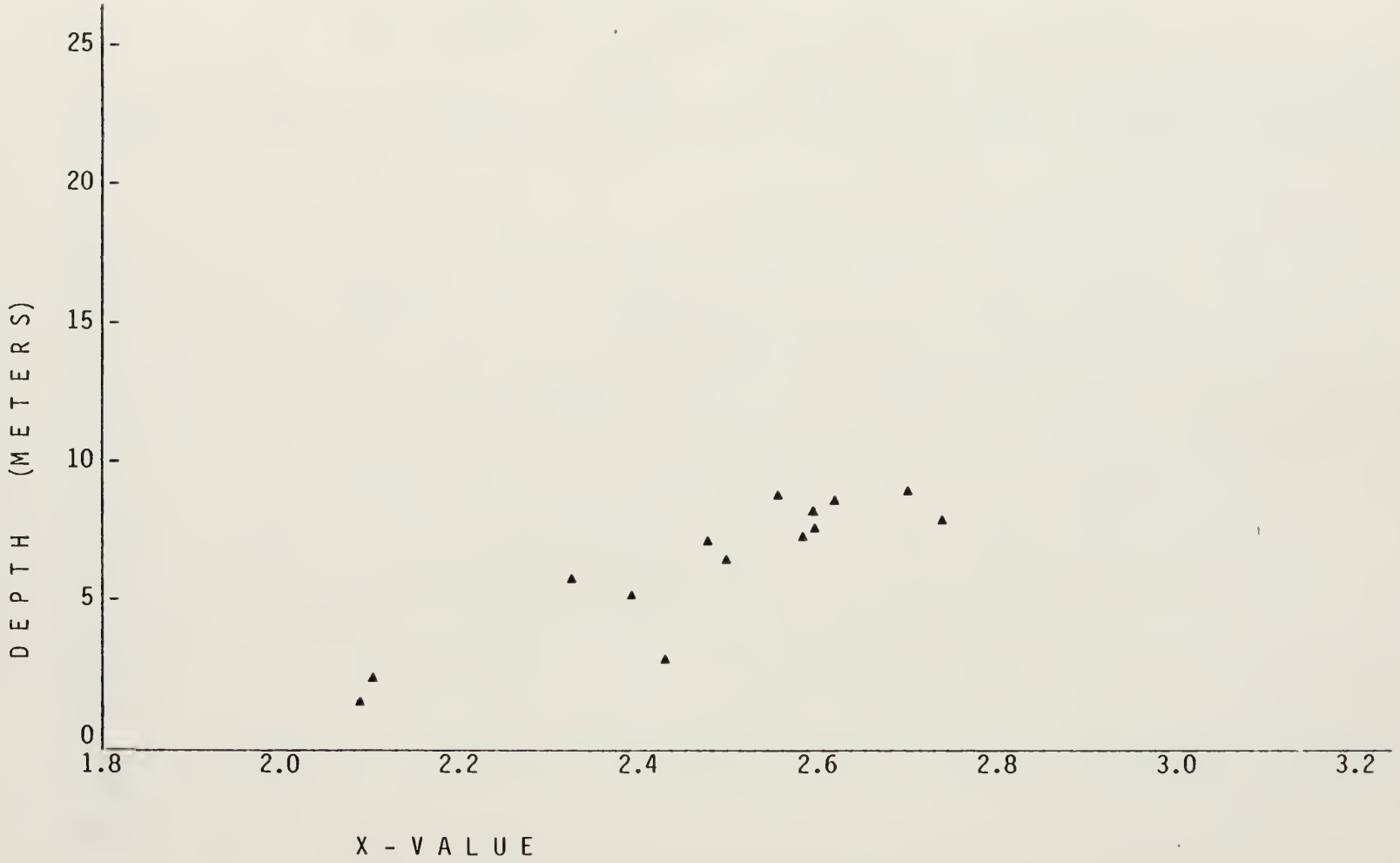

Figure 7. Plot of Log Reflectance Parameter (X) vs. D for Site 3 Test Sample

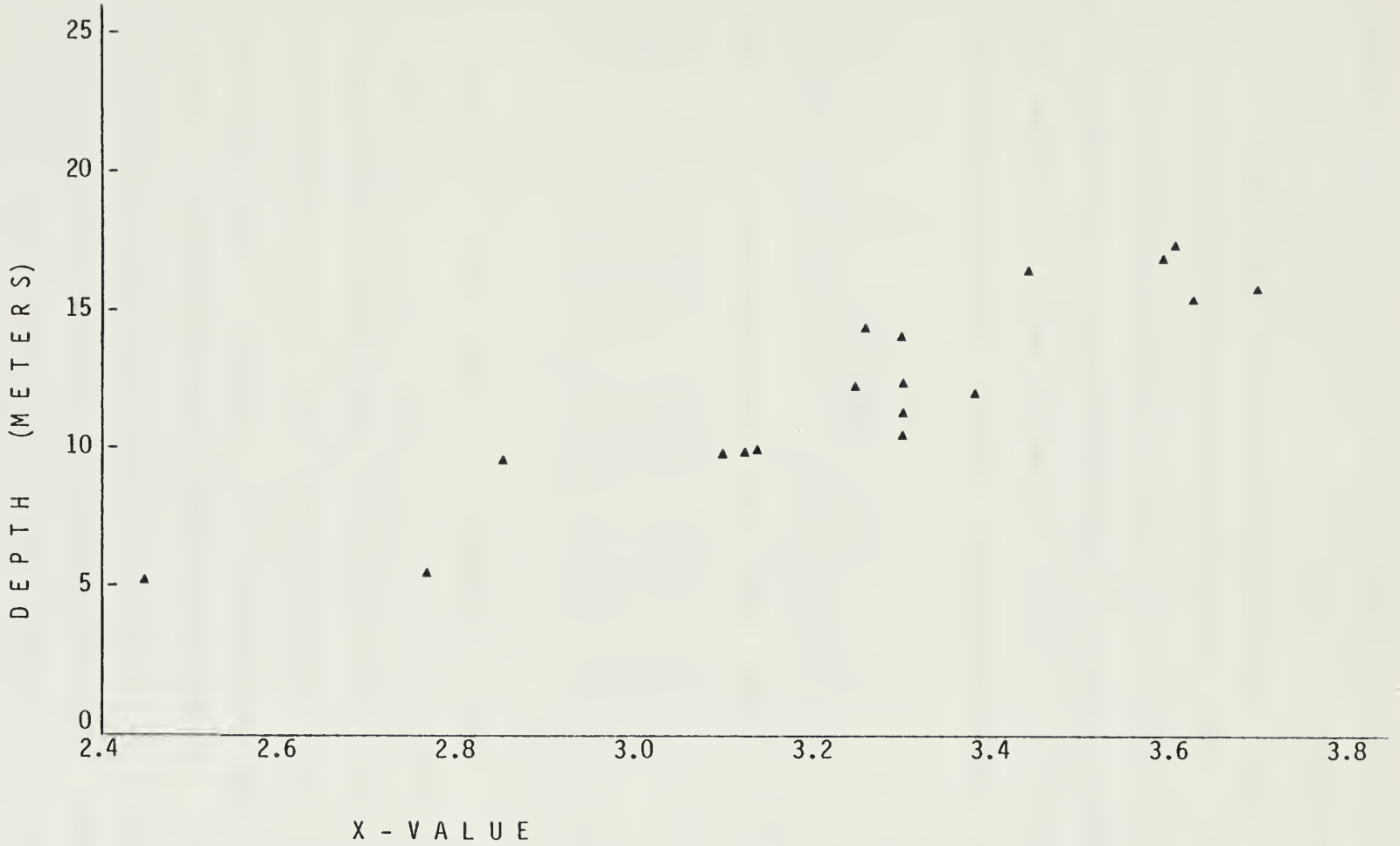

Figure 8. Plot of Log Reflectance Anomaly (X) vs. D for Site 4 Test Sample

presence of a linear correlation is strongly suggested in each figure.

The following statistics were computed for each sample set: 1) the squared correlation coefficient R^2, 2) the standard deviation of the residuals S_D in m, and 3) the standard error of prediction S_P in m. These values are presented in Table 5, together with the linear regression coefficients (A and B) and the derived optical parameters (K_4 and R_{b4}).

TABLE 5
Results of Analysis for Test Areas 1 and 2

SITE(S)	K_4 (m^{-1})	R_{b4}	A	B	R^2	S_D (m)	S_P (m)
1	.041	0.204	-24.107	-14.891	0.88	1.90	3.86
1 & 2*	.052	0.258	-16.482	-11.869	0.79	1.26	2.27
3	.045	0.237	-20.642	-11.202	0.79	0.56	1.65
4	.043	0.236	-25.228	-11.548	0.83	1.08	1.92
3 & 4*	.043	0.234	-29.993	-12.879	0.74	1.15	1.84

(*Combined)

The depth predictions in Test Area 2 (Sites 1 and 2) were consistently more accurate than in Test Area 1 (Sites 3 and 4). The largest S_P computed for Test Area 2, 1.92m (Site 4), was 15 percent lower than the 2.27m S_P computed for 3.86m S_P computed for Site 1. The S_D for each of the three analysis performed in Test Area 2 were likewise consistently lower than those computed for Test Area 1.

The computed statistics also indicate the effect of increasing sample size in each test area. In Test Area 1, the S_P improved from 3.68m to 2.27m by combining the sample

from Sites 1 and 2; similarly, S_D was lowered from 1.90m to 1.26m by pooling the data from the two sites. In Test Area 2, no trend emerges as a result of combining Sites 3 and 4. The resulting S_D was lower than that computed for Site 4, but was higher than that computed for Site 3. The R^2 and S_D values computed for the combined Sites 3 and 4 (0.74 and 1.15m) were actually degraded from the values computed for each of these statistics for Sites 3 and 4 separately.

There were also significant differences in the homogenity of the two test areas. The optical characteristics (derived from the coefficients A and B) for Sites 3 and 4 are more internally consistent than are those for Sites 1 and 2. The values for K_4 range from .041 to .052 in Test Area 1, but only vary from .043 to .045 in Test Area 2. Similarly, R_{b4} values range from 0.204 to 0.250 in Test Area 1 and from 0.234 to 0.237 in Test Area 2.

The analysis of results presented in Charpter IV will address the relative accuracies achieved in the two test areas, the homogeneity of the optical factors, and the effect of varying sample size in each test area. Assuming these factors are related, the site dependence of this technique and the extent of the error analysis necessary for areas of varying homogeneity is indicated. These issues are discussed in the Cost Benefit Analysis presented in Chapter IV.

IV. DISCUSSION

A. ANALYSIS OF RESULTS

The linear regression analyses performed on the Great Bahama Bank and the West Florida Shelf samples indicate significant differences between the two test areas. The results obtained from Test Area 1 are characterized by internally inconsistent values for the optical parameters, K_4 and R_{b4}, relatively inaccurate depth prediction (compared to Test Area 2), and some improvement in accuracy with increased sample size. Test Area 2 yielded consistent optical values, relatively accurate depth prediction, and no increase or decrease in accuracy with varying sample size. The interpretation of these kinds of differences is an important step in determining the conrol required to achieve desired accuracies.

The magnitude of the differences in the K_4 and Rb_4 values derived for the two analyses performed in the Great Bahama Bank Test Area indicates the need to acquire more representative test samples. The strong tendency of the model to over-estimate depths in shallow waters (less than 11m) in both analyses, emphasizes the need for improving the accuracy level. Lyzenga and Polycn (1979) obtained similar results, as indicated by a mean bias of -1.29m, using a single bottom reflectance value for several stations, further emphasizing the dangers of not accounting

for inhomogeneities. For this test area, the accuracy of the predictions might be improved by either acquiring a larger combined sample, or by acquiring larger local samples from each site and performing separate linear regressions. Lyzenga and Ploycn's results for the same area support the latter alternative. The wide range in the bottom reflectance values measured (0.10 to 0.24) is a good indication that no single set of coefficients will ensure accurate depth prediction for the entire Bahamas Photobathymetric Test Range. This result suggests: a) that spatial trends in optical properties be determined using concurrent ground truth data, and b) that a procedure for estimating a "lowest probable bottom reflectance" which will bias MSS depth errors towards relatively safe underestimates. These suggestions will be developed in more detail in the next section and in Chapter V.

The similarity in the optical parameters derived for each of the three West Florida Shelf sample sets indicates highly homogeneous conditions over the entire test area. These optical conditions, and the smoothly varying bottom topography of the West Florida Shelf, combined to yield greater accuracy than was achieved in the Great Bahama Test Area. The accuracy achieved by combining samples from the two sites was higher than that achieved with the Site 4 sample but less than that with the Site 3 sample. This result was anticipated since, in a nearly homogeneous

environment, a relatively small sample may be just as representative of the entire population as a larger sample would be. Likewise it is obvious that, in this instance, a sample collected from a single site is potentially as good a predictor of depths throughout the test area as a sample collected from several sites.

The differences between the results obtained from the two test areas are seen to be a result of the differences in the degree of homogeneity in each area. In Section IV.B these results will, in turn, be used to assess the impact of various optical conditions upon the usefulness of single band prediction techniques.

B. ERROR IMPACT ANALYSIS

1. Introduction

The error associated with water depths derived from MSS imagery is the primary factor governing the scope of their use in a bathymetric charting program. The requirements for depth data intended for use in nautical chart compilation are more stringent than for those used in pre-survey evaluation. It is also apparent, from the results of the two case studies performed for this thesis project, and from the results of Lyzenga and Polycn (1979), that the quantity of control data required to achieve a set level of accuracy will vary from area to area.

2. Sources of Error in Depth Estimation

Variations in bottom reflectance, water clarity, and/or any other optical values assumed constant, will contribute errors in depth prediction. In the Bahamas Test Area, the variation in bottom reflection was identifiable as a principle error contributor. This case is probably typical of coral reef environments, which exhibit marked variability in bottom vegetation. Usually vegetation acts to reduce bottom reflectance, especially relative to that of the bright sandy bottom typical of the Bahamas. Therefore, if the average bottom reflectance to be used in an area has been measured over a relatively vegetation-free bottom, increased vegetation at any location will result in overestimated depths. Underestimation of depths occurs if the "average" bottom reflectance is measured over an area with more than the normal amount of vegetation.

The obviously dangerous risks associated with overestimated depths suggests that a procedure be developed to determine a "lowest probable bottom reflectance", which will bias errors in MSS depths towards less dangerous underestimates. Future research should be initiated to standardize such a "safe bias" procedure, and to quantify the associated probability of overestimated depths being greater than 0.3m.

Although the Bahamas test results did not so indicate, a second possible error source in areas of active

reef building is the variation in water clarity caused by the presence of plankton. Planktonic activity increases the attenuation of light, thereby reducing the bottom return; this results in overestimation at all depths.

The results summarized in Table 5 confirm the assumption that the bottom reflectance in the Florida Test Area is more spatially uniform than that in the Bahamas. It was expected however, that there might be some noticeable difference in water clarity between Sites 3 and 4. Site 4 is located nearer the mouth of the Tampa Bay, and it would not have been surprising if either or both bottom reflectance and water attenuation would have changed systematically between open coast and estuarine environments. However, systematic variations were not evident in either K_4 or R_{b4}.

C. IMPACT OF ERRORS ON POTENTIAL USES

1. Chart Evaluation Using MSS Derived Bathymetry

Zoned-depth maps prepared from multispectral imagery may be used to evaluate existing charts. Initially, the boundaries between depth zones could be compared to bathymetric contours to detect major topographic changes over time. Because patterns, rather than isolated soundings are being compared, the absolute vertical accuracy requirements are less stringent than for direct mapping using MSS alone.

Although it would be desirable to compute depths from local groundtruth, this will usually be impractical since the survey data being evaluated is questionable, and K_4 and Rb_4 will generally not be known to any useful degree of accuracy.

However, even visual comparisons of zones of relative brightness on MSS imagery with depth contours have proven to be useful. Such comparisons have resulted in detection of at least one uncharted marine hazard which was later verified (Hammack, 1977). At the very least, the zoned depth map can be used to produce a relative evaluation of chart coverage, for better long range survey planning.

2. Use of MSS-Derived Depths as a Pre-Survey Planning Tool

The purpose of pre-survey planning is to determine the most cost effective procedure for accurately gathering adequate hydrographic data for a prospective site. When the data available from a particular survey site are unreliable or incomplete, MSS coverage can provide a valuable planning tool. DMAHTC has prepared several relative depths maps for use by NAVOCEANO in the planning stage (Joy, 1981). Boundaries were defined to correspond to depth contours used on nautical charts. Typically 0.5m, 10m, and 20m isobaths, and if high tide and low tide images are both available an "uncovers" curve, were portrayed. Comparison

of corresponding isobaths plotted on each chart type indicated the degree of change in bottom topography since the last survey. Previously undetected shoals were indicated on the MSS-depth map, and some charted dangers were confirmed; both occurrences represent cases requiring special attention during the next survey. Because undetected shoals represent danger to survey ships, as well as to normal shipping, detection of doubtful depths alone may justify the expense of preparing depth maps from MSS imagery.

The relative depth curves depicted on the initial maps prepared for NAVOCEANO were based almost entirely on variations in brightness (photointerpretation techniques were used when possible to classify bottom types). Although no accuracy level was attached to these products they were found to be useful planning tools.

Although depths predicted from the algorithm described in this study are potentially more reliable than "raw" MSS4 counts, the cost of obtaining the necessary ground truth does not appear to be justified for the purpose of pre-survey planning.

For many unsurveyed, or insufficiently surveyed areas, estimates of water clarity and bottom type can be made with sufficient accuracy to make use of MSS depth data in prioritizing and planning surveys. The inability to define a level of accuracy does not preclude these

applications entirely. The potential benefits include more informed risk analysis in deciding where charts most need to be updated because of possible dangers, and more informed pre-survey planning to ensure that possible dangers are investigated and developed thoroughly. These benefits easily translate into safer waters.

3. Use of MSS Imagery as a Direct Source of Bathymetric Data

Depth information appearing on nautical charts must be both accurate and reliable. The errors associated with depth prediction in this and previous studies exceed the errors allowed for conventional survey data (0.3m for depths between 0 and 20m, and 1.0m for depths between 20 and 100m) (Umbach, 1976). Because these studies were conducted in locations with above average bottom reflectance and/or water clarity, lesser accuracies may be expected or achievable in less ideal sites.

Also the risk of overpredicting depths, especially in very shallow waters, is unacceptably high. All results of the present and previous work indicate strongly that MSS estimates of depth are too unreliable to be used as a direct independent basis for bathymetric maps. Practical charting applications will be restricted to techniques using MSS imagery together with other, independent sources of bathymetric data.

4. Use of MSS-Derived Depth Data as an Interpolation Tool

The accuracies indicated by this and previous studies (Lyzenga, 1981) suggest the possibility of using MSS-derived depths for interpolating between survey track lines in some areas. The potential usefulness of the technique in a particular candidate survey site can be evaluated through pre-survey analysis of MSS imagery. This survey planning application of MSS images is discussed above and in Chapter V.

Conventional survey track lines are planned at specified intervals to insure complete coverage and to optimize use of ship time. By supplementing shipboard survey data with a matrix of accurate and reliable depths produced from MSS imagery, it would be possible to widen track lines while still meeting data acquisition requirements. Optical measurements taken at specified intervals during the survey would be used to compute the coefficients required for predicting depths with MSS data. Using commercially available microcomputers and submersible optical instruments, a towed optical measurement package can be configured to obtain continuous along-track measurements with only minimal operator attention during routine surveys. If K_4 and R_4 are measured in situ along each survey trackline, it will be possible to constrain the regression fit to account for spatial trends in ocean

optical properties and bottom reflectance. With such spatially adjusted constraints, previous work (Warne, 1978) has demonstrated that rms accuracies of less than 1m can be expected (additional research must be done to determine whether accuracies approaching 0.3m are feasible). Additionally, use of spatially adjusted minimum bottom reflectance can reasonably ensure that errors in the depth interpolation field are safely biased underestimates.

The accuracy level of the interpolated depths would be calculated by comparing the predicted depths along each track line with the reduced sounding data taken along randomly interspersed intermediate survey tracklines. This method of obtaining a reserve sample, and determining rms errors in interpolated soundings, can be easily extended to evolve a procedure of successive refinement of trackline spacing. If the initial rms accuracy were acceptable, the initial trackline spacing would be accepted and the survey pronounced completed for that area. If not, the survey pattern would be tightened by filling in tracklines half-way between the original ones, with a reserve sample obtained at a few randomly interspersed quarter-interval lines. The procedure would be thus iterated until an acceptable accuracy level was obtained.

The design of an experiment to test the feasibility of achieving an accuracy of 0.3m in MSS-interpolated depths must be quite different than that common to the studies

conducted and reviewed in the present project. All results presented here pertain to depth estimates calculated from Equation (6) using a single set of regression coefficients for a given site. In the interpolation scheme, the coefficients must be adjusted continuously according to local correlations between upwelled radiance and water depth, as constrained by the corresponding in situ measurements of K_4 and R_4; the amount of along-track data to be included in determining local coefficients must be evaluated experimentally in the context of a standard optimal interpolation method. Development of these concepts in more detail is left for future projects.

The evenness of the bottom and the estimated accuracy level of the predicted depths would be used to determine the feasibility of using this technique in each site on a local basis.

D. COST BENEFIT ANALYSIS

Once an error analysis has justified using MSS or TM derived depths for interpolating between tracklines, several factors combine to reduce the cost of the survey.

The principal savings results from a reduction in the number of days required for nearshore (i.e. within the 100m depth contour) survey coverage. (This is also the most dangerous area to survey). Nearshore surveying (when done by conventional means) is also very time consuming, despite

the relatively small area involved. The greater density of data required to adequately develop areas within the 100m depth curve, (500m spacing versus 1000m spacing outside this zone) requires extensive boat time and processing time. It is not unusual for the nearshore surveying and processing to take longer than the offshore survey of much larger areas. This reduces the "mother" ship to a support vessel, rather than a data acquisition vessel.

The benefits to be realized from the use of MSS depth interpolation fields are cost savings which scale directly as the ratio of reduced survey track miles to survey miles at standard trackline spacing, less a relatively small overhead associated with acquisition and analysis of Landsat MSS imagery and ocean optical properties. A reasonable estimate for acquiring and analyzing a single MSS image is $3000.00, and up to five images might be required for a single 100km X 100km survey site (considering cloud cover and tidal stage variations). Assuming a complete towed optical system per unit cost of $50,000 and an average useful life of 1000 operating days, the optical package would add only $50 per day to survey vessel costs; this is an insignificant increment compared to (conservatively) estimated costs of order $10,000 per operating day for Class-I survey vessel. Using these figures, if a 50 percent reduction in trackline spacing were achieved through use of MSS depth interpolation in a

site requiring ten ship days at conventional spacing, the cost savings would be approximately $35,000. Assuming only ten candidate survey sites per year have ocean optical properties and bottom reflectance characteristics which are suitable for this technique, the annual savings would amount to approximately $350,000. At a very plausible assumed average reduction of 75 percent, the pre-survey and annual savings would be $60,000 and $600,000. These estimates are admittedly speculative, but they are reasonable speculations and show that significant benefits can be anticipated if MSS depth interpolation accuracies of approximately 0.3m can be realized.

E. RELATED TECHNOLOGICAL DEVELOPMENTS

Recent advances in remote sensing technology are expected to improve the accuracy levels of satellite bathymetric data. The most significant advance in multispectral imaging technology is the Thematic Mapper (TM) aboard Landsat D. This system offers improved spatial resolution (30m versus 96m using the MSS) which will reduce the smoothing of bottom features over each field of view. Spectral resolution has also been improved from the MSS 0.1μm band to approximately a 0.07μm. Therefore, the wavelength dependent terms in the optical model are apt to be more representative of the radiance sensed by a particular band. Additionally, the TM carries two bands

suitable for depth prediction: one, centered at 0.48μm, (closely corresponding to the maximum transmittance of relatively clear water) and the other centered at 0.58μm. This redundancy can be used to compute pixel by pixel values for the bottom reflectance, as well as the water depth, which was previously possible to only a few m with the MSS Band 5. Also, depths may be computed with greater digital resolution because of the instrument's finer radiometric resolution. These improvements, combined with in situ optical measurements, should ensure predicted depths accurate and reliable enough to serve as interpolation data in many circumstances.

The development of the Multispectral Active/Passive Scanner (MAPS) can provide an alternate source of water depth data. This system may be mounted on fixed wing aircraft and has the advantage of providing its own optical ground truth. While the passive scanner records reflected radiance in several blue-green bands, a pulsed laser (also in the blue-green wavelengths), is used to determine the optical properties of the water column and bottom. With these param, the passive data can be used to derive information to depths as great as 40m (DMAHTC, 1984).

Other applications of laser technology include the Hydrographic Airborne Laser Sounder (HALS), another aircraft system, which can provide high density (9m intervals) sounding data across a swath 200m wide. This

system has demonstrated the capability to measure depths within IHO accuracy standards (DMAHTC, 1984). This system might be used to quickly acquire the control depths necessary to evaluate the accuracy of the MSS or TM, reducing still further the burden on survey launches.

The use of Synthetic Aperture Radar (SAR) imagery in conjunction with MSS or TM imagery is expected to provide more detailed bathymetric information for pre-survey analysis and planning. SAR is an active sensing system operating in the microwave range. It has been observed that certain surface features observed on SAR imagery (surface gravity wave refraction patterns, internal waves, and anomalous backscatter patterns) are tied to distinctive bathymetric features (Lodge, 1983). Because SAR is an active system, it's operation is not dependent upon weather conditions. This can be used to great advantage when compiling pre-survey bathymetric charts in each area where the use of MSS or TM data is often limited (e.g., in the sub-tropical convergence zones which are often cloud-covered). The potential application of SAR imagery and multispectral data used jointly is further discussed in Chapter V (Recommendations).

V. CONCLUSIONS AND RECOMMENDATIONS

From the information presented in the preceding chapters, it is clear that quantitative bathymetric maps can be prepared from Landsat MSS images of hydrographic survey sites characterized by transparent waters and a highly reflective bottom. Used as an independent data source, with regression coefficients fit to control depths measured at only a few locations, rms errors typically ranged from 1 to 2.5m under appropriate optical conditions. The primary source of error is spatial variability in ocean optical properties and/or bottom reflectance. This accuracy level is adequate for use of MSS imagery as a tool in bathymetric chart review and revision (Section IV.C.1), and for pre-survey planning (Section IV.C.2), but falls far short of the 0.3m accuracy standard for soundings less than 20m (Umbach, 1976). The conclusion is inescapable that bathymetric charts derived from remotely sensed multispectral images alone are far too inaccurate, even under ideal optical conditions, to obviate the need for conventional in situ hydrographic surveys (Section IV.C.3). However, significantly improved accuracy may be expected if MSS images are instead used to interpolate depths between concurrent ship survey tracklines at wider-than-normal intervals. Further experimental research is needed to determine whether 0.3m depth accuracies can be realized,

but if so, the MSS interpolation technique will prove to be extremely cost-effective. The following sections outlined recommended procedures for integrating Landsat MSS-derived depth products into a bathymetric charting and surveying operational demonstration program.

A. RECOMMENDED CHART REVISION AND SURVEY PLANNING PROCEDURES

Figure 9 illustrates schematically a recommended sequence of procedures through which MSS images may be routinely incorporated into long-range hydrographic resource planning and interim chart revision. The construction of the preliminary bathymetric "working chart" would first require obtaining a combination of multispectral (MSS now and TM when available) and SAR imagery for each area in which DMAHTC is the responsible authority. As indicated, data for each area would be acquired in order of priority. This imagery would be used to depict relative depth zones and to delineate dangerously shallow waters, as clearly as possible. The use of SAR imagery is recommended for identifying areas which exhibit manifestations of shoals; these areas can then be more carefully investigated using the Landsat imagery. The working bathymetric chart should also contain annotation pertaining to suspected hazards or anomalies which could

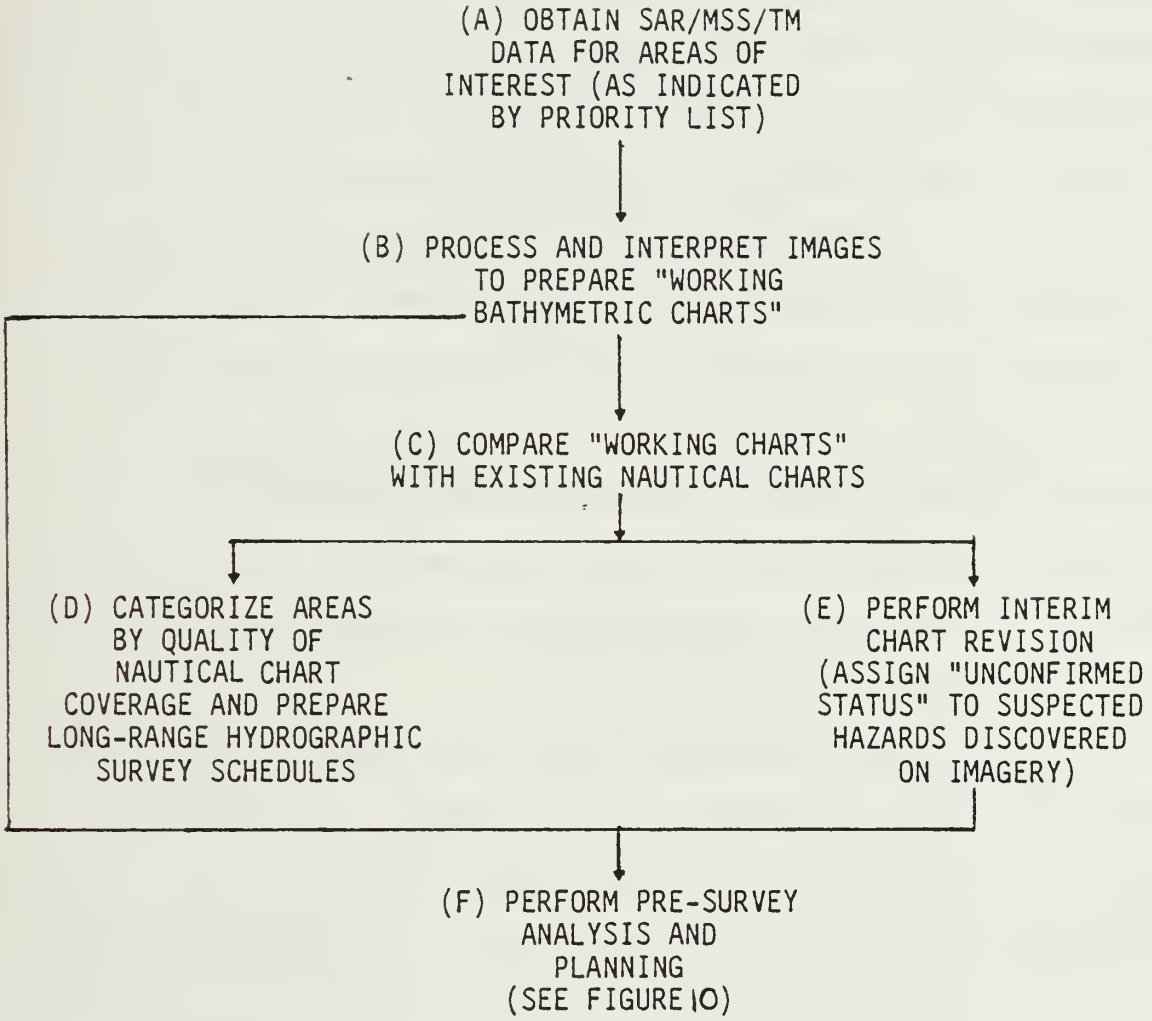

Figure 9. Use of Multispectral Imagery in Chart Revision and Long-Term Planning

not be clearly interpreted or delineated with either the multispectral or SAR imagery.

As shown in Step C, the completed working chart is intended to offer a basis for evaluating how well the available chart coverage represents the current bottom topography of an area. This evaluation would provide input to planners to further categorize areas of equal priority. In Step D, this additional input will ensure that those high priority areas most lacking in quality hydrographic data receive first attention. The information appearing on this working chart would also be used to update the current nautical charts, until the area had been properly re-surveyed. The use of "uncomfirmed hazard" and "position approximate" labels would differentiate this information from controlled survey data while still warning mariners of possible dangers.

The bathymetric working chart and updated nautical charts are also intended to be useful tools in the pre-planning phase of a survey, as illustrated by the arrows leading from Steps B and E to Step F. This concept is more fully developed in the next section.

B. BATHYMETRIC SURVEY ENHANCEMENT USING MSS DEPTH INTERPOLATION

Figure 10 illustrates a recommended sequence of procedures for utilizing MSS images as depth interpolating fields in bathymetric surveys in sites shown by pre-survey

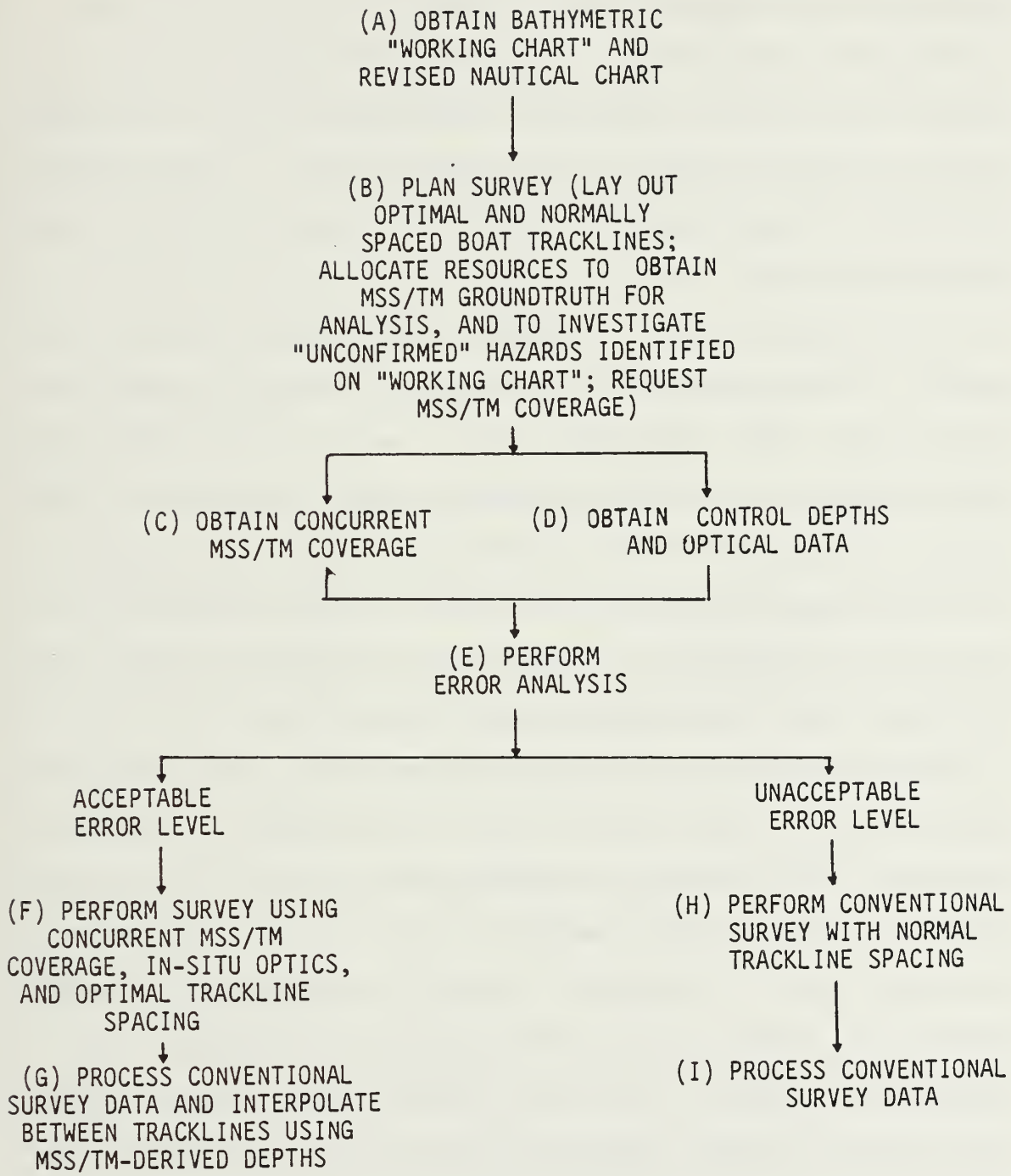

Figure 10. Integration of Multispectral Imagery into a Hydrographic Survey Program

analysis to be suitable in terms of ocean optical properties and bottom reflectance. The basis for this approach was discussed in Section IV.C.4.

For favorably rated areas, the first step, shown in Step A, is to obtain the preliminary working chart and the revised nautical chart, which would have already been prepared. These would be used, in Step B, to plan the nearshore survey.

Step B (Figure 10) encompasses three major planning tasks. First, two sets of survey tracklines would be prepared for the nearshore areas: one set (designed to take advantage of the depth matrix supplied by MSS or TM imagery) would be spaced at wider intervals than those used in conventional surveys; a second normally spaced set, would also be prepared in the event the error analysis is Step E produced unacceptable error levels.

The second planning step would involve the allocation of resources for those tasks other than regular trackline surveying. This amounts to investigating those unconfirmed hazards detected in the imagery, or previously reported by mariners, and obtaining optical measurements and groundtruth (Step D) for the analysis in Step E. The information depicted on the working chart should make locating potentially hazardous areas more efficient and thorough. Not only is it more likely that dangerous areas would be properly investigated, but the entire nearshore

survey operation would be safer with more of these areas identified ahead of time.

The third step involved in the planning phase would be to request MSS or TM imagery to be taken at the time scheduled for acquisition of ground truth and optical measurements. Scheduling for this task would be driven by the 18-day coverage cycle of the Landsat satellite, by the availability of boats and crew to obtain groundtruth, and by weather conditions. Steps C and D represent the simultaneous acquisition of all data required to perform a thorough error analysis in conjunction with the survey. Soundings and optical properties might best be measured by a single boat dedicated to this task. Before the survey proceeded from one site to the next, this boat could be sent ahead to acquire the necessary data. The sooner the data are in hand the more easily necessary changes could be planned before actual survey operations were well underway. With modern microcomputers, it is possible to take optical measurements using towed instruments, with minimal operator interface; a two or three man crew could easily obtain the necessary data sample.

The analysis to be performed in Step E would be similar to that described in Section III.C. First the depth measurements would be randomly divided into two samples. A test sample would be used to derive the coefficients A and B (from Equation 6) required to predict depths. From

these, values for K_4 and Rb_4 would be derived and compared to the in situ optical measurements; if necessary, the coefficients would be locally adjusted to these measurements. The resulting coefficients would be used to predict depths for each X value (computed from the Landsat counts per Equation 2) in the control sample. An unacceptable error level in Step E would automatically require switching to conventional survey procedures. If the error level were acceptable, nearshore survey operations would proceed with boats following widened survey tracklines and carrying towed instruments for measuring water clarity.

C. RECOMMENDATIONS

In summary, the results of the literature review and case studies performed in this thesis project lead to four key recommendations related to use of visible wavelength multispectral imagery in an operational bathymetric mapping program:

1. Procedures should be implemented for routinely using Landsat MSS images in the planning and management of operational bathymetric survey and charting programs. The benefits to be derived from interim chart revision and pre-survey and pre-survey planning using MSS and SAR-derived depth manuscripts are well worth the small expenditure of resources required for processing and compilation.

2. Research should be carried out to develop a quantitative procedure for determining "lowest probable bottom reflectance" values for use in all MSS depth algorithms. The motive for this procedure is to bias errors towards safe underestimates, and to reduce the probability of dangerous depth overestimates to a low value. A primary objective of experimental research in this area should be to quantify the probability of depth overestimates exceeding 0.3m (the accuracy standard for depths less than 20m) and establish associated confidence levels.

3. New experimental research should be initiated to determine accuracies associated with using an MSS image as a basis for interpolating depths between in situ survey tracklines, with spatial trends in ocean optical properties constrained by in situ measurements along each trackline. Existing data from previous experiments are not properly distributed for this purpose, although an initial assessment could be performed by modifying the present case study of the Florida Test Area to interpolate between charted survey depths at varying trackline spacing. As was discussed in Section IV.D, significant cost savings can be anticipated even if only ten or so survey sites per year have ocean optical properties and bottom reflectance suitable for use of MSS depth interpolation; the potential

savings are large enough to justify placing a high priority on quantitative evaluation of this particular approach.

4. In contrast to the promising potential for depth interpolation using MSS images, all results of the present study suggest that MSS derived depths are not sufficiently accurate to serve as a direct, independent basis for bathymetric mapping. Due to spatial variability in optical properties, error levels 1m (or more) greater than the 0.3m allowable level are expected. Therefore, it is recommended that research and development efforts de-emphasize (or even abandon) this extremely demanding goal and focus on the more plausibly achieved applications emphasized above.

Finally, it is recommended that future work in this topic area be organized with a formally established technical development and operational demonstration program. Obviously, many of the technical questions implied in the above research can be approached through uncoordinated, stand-alone experiments. To convincingly establish the cost effectiveness and operational utility of these techniques, however, a comprehensive program of carefully designed demonstration surveys is considered essential.

APPENDIX A. LANDSAT SATELLITE SERIES AND THE MULTISPECTRAL SCANNER

The following general discussion of the Landsat Satellite series and the Multispectral Scanner (MSS) applies to Landsat-1 through Landsat-3. Landsat-4, launched on July 16, 1982, is an operational satellite, whereas the first three were experimental. Furthermore, Landsat-4 has different orbital characteristics and imaging systems than the previous satellites, and will require more complex processing techniques.

1. LANDSAT SERIES - CHARACTERISTICS

The Landsat series of satellites has served primarily as a research and development tool to demonstrate the usefulness of remote sensing from space to various earth science applications (Warne, 1978). Landsat-1 (initially named ERTS-1) and its two successors, Landsat-2 and Landsat-3, were launched in 1972, 1975, and 1978, respectively; the durability of each satellite has resulted in nearly continuous coverage since the initial launching in 1972 (Taranik, 1978). Although post-processing techniques have generally lagged behind the remote imaging technology, the variety and quality of users has continued to increase with each mission. Landsat-4 has incorporated technology designed to accommodate many of the common user

requirements which have developed through exploitation of data from earlier missions (Taranik, 1978).

Each satellite was launched into a near-polar, sun-sychronous orbit, at an average altitude of 900km. The angle between the sun, center of the earth, and the satellite is maintained at 37.5 degrees, and the orbital plane is inclined 99 degrees, as measured clockwise from the equator. These orbital characteristics are designed to insure repetition of suitable sun-illumination conditions. The average period of orbit is approximately 103 minutes, offering repetitive ground coverage, by individual satellites, of each 185 by 185 km area, every 18 days (Taranik, 1978).

2. LANDSAT MULTISPECTRAL SCANNER

Each satellite was equipped with a Multispectral Scanner (MSS) and a Return-Beam Vidicon (RBV) camera system as part of its imaging payload. The MSS contains six detectors in each of the following four wavelength bands:

BAND	RANGE (μ)	TYPE OF RADIATION
4	0.5-0.6	blue-green
5	0.6-0.7	visible red
6	0.7-0.8	invisible reflected IR
7	0.8-1.1	invisible reflected IR

(An additional 5th band, which detects thermal infrared radiance, was installed in the Landsat-3 MSS). The RBV camera system has not been widely applied to bathymetric mapping and so will not be discussed further here. Details of the RBV camera system are presented in Taranik (1978) and Slater (1980).

Each detector in MSS Bands 4-7 samples the reflected radiance over a 79 by 79m area every 9.95 milliseconds through a sweep angle of 11.6 degrees; 390 scans (of each of the six detectors) are formatted into one 34,225 square kilometer scene, for each of the four bands. (USGS, 1979)

3. SIGNAL PROCESSING TO PRODUCE COMPUTER COMPATIBLE TAPES

The following discussion refers to pre-1978 procedures, utilizing the NASA Data Processing Facility (NDPF). With the introduction of NASA's Image Processing Facility (IPF) in 1978, other radiometric and geometric corrections were applied in the production of standard high density computer Compatible Tapes (CCT's).

The reflected radiance received by each detector is initially registered as a measure of voltage. The Landsat MSS can record radiance in either a low gain (normal) or a high gain setting. In the high gain mode, each signal in Band 4 and 5 is amplified by a factor of three, which effectively reduces discrimination between the higher

radiance levels while increasing the resolution in the lower levels (USGS, 1979).

The analog data in each band (except Band 7) is then "compressed" so that each voltage level is assigned a value on a scale ranging from 0-63 (see diagram); this produces a quantization which more nearly matches the inherent MSS photomultiplier noise in each band (USGS, 1979). The algorithm applied is non-linear, and in effect, results in a compression of the higher radiance levels and an expansion of the lower radiance levels.

High gain is preferred for water depth determination. In water depths greater than 10m, bottom reflectance contributes only small radiance anomalies above the deep water radiance $L_{\infty 4}$ (Ch. II). The improved radiometric resolution at low radiance levels is virtually essential if these anomalies are to be detected.

Upon reception, the compressed digital values are decompressed to fit a linear scale ranging from 0-127 counts. Because of the non-linearity of the compression algorithm, and because of the inherent differences between compressing an analog signal into a digital value and the subsequent decompression of that digital value, the lower level signal values become compacted into relatively few discrete "steps", or counts, with unused counts at the higher levels (referred to as forbidden numbers) (Warne, 1978).

Prior to 1978, two additional radiometric corrections were made, by NASA, to correct for variations in the response of each detector in each band (Lyzenga and Polcyn, 1979).

In addition to radiometric corrections, bulk processing at the NASA Data Processing Facility included geometric corrections to; 1) normalize the length of the scan lines, 2) register the four bands to one another, and 3) correct for variations in satellite altitude and attitude as recorded by on-board equipment (USGS, 1982). Each corrected image was stored on 800 or 1600bpi "band-interleaved by pixel pair" format. (This description applies to pre-1980 Landsat MSS data; procedures and formats have been modified since then).

APPENDIX B. NAVIGATION OF LANDSAT SCENES

Navigation of imagery produced by a scanning satellite sensor, such as the Landsat MSS, refers to the development of an algorithm for assigning map coordinates (e.g. latitude and longitude) to image pixels. Selection of a suitable navigation technique is dependent upon 1) the accuracy required from the algorithm, 2) the availability of resources, particularly suitable processing facilities and appropriate firmware and software support, and 3) time constraints. High accuracy standards require CCT's which have been geometrically corrected for distortion arising from rotation beneath the satellite, spacecraft velocity changes, satellite altitude and attitude variations and scan skew. The most accurate methods involve modeling the instantaneous sensor position by measuring the displacement of image identifiable ground control points from their true positions on an appropriate projection; from these measurements, a mapping function is derived which allows geographic coordinates to be "mapped" onto the input image. The input image is then re-sampled (within the vicinity of the mapped position coordinates) to assign a value to the mapped position of the particular coordinates, since the position of the coordinates on the input image will not usually coincide exactly with the center of any one pixel.

Although the above procedure is the most accurate, Landsat tapes which were produced by bulk processing were not corrected in this fashion. Instead, the bulk processor utilized on-board monitors to record detectable variations in the altitude and attitude of the Landsat platform; geometric corrections are then automatically made in response to this data. Two further geometric corrections are made to a) normalize the scan line lengths, and b) to co-register the four bands. The accuracy of this procedure is sufficient for the present application.

The navigation procedure used here, models the change in latitude and longitude from one pixel to another along each scan line, and from subsatellite point to subsatellite point between different scan lines. Based upon the known coordinates of the control points and the subsequent calculation of the sub-satellite points of the scan lines in which each control point was located, the change in latitude and longitude, from any control point to its scan-line subsatellite point, and thence to any point on any scan line could be computed. The procedure was based upon a plane sailing approximation, i.e., that the areas of concern in each of the two scenes could be treated as flat surfaces for the purposes of computing differences in latitude and longitude. This is a generally accepted assumption for marine navigation problems involving only small changes in latitude and departure over relatively

short distances (under a few hundred miles) (Bowditch, 1977). Computation of the latitude of the point of arrival can be computed by a direct solution of the plane triangle; the computation of longitude change requires scaling by the cosine of the mid-latitude (along which all changes in longitude are assumed).

The application of this procedure to Landsat MSS images is described below.

Step 1.

As an initial evaluation, to determine whether or not the bulk processed tapes of the Bahamas and Florida areas were sufficiently corrected for use with the proposed navigation algorithm in the project areas, a plot was made of the subsatellite points of each scan line containing a control point. Over the distances covered by each test area (approximately 15 nautical miles north-south in the Bahamas test area, and 37 nautical miles north-south in the Florida test area), it was assumed that the subsatellite points, for those portions of each scene actually used, would lie along a straight line (as plotted on a Mercator projection).

The maximum deviation from a "best-fit" line for any of the plotted subsatellite points, in both Bimini and Florida, was well within the error level associated with measuring control point position and the subsequent plotting of subsatellite points.

The following equations were used to calculate the latitude and longitude of the subsatellite point (P_o) of each scan line (ℓ) containing a control point:

$$LAT(P_o,\ell_o) = LAT(P_c,\ell_c) + d(P_c - P_o)\,SIN\,\phi_{SAT}, \quad (10)$$

$$LONG(P_o,\ell_o) = LONG(P_c,\ell_c) - (d(P_c - P_o)/COS\,\bar{L})\,COS\,\phi_{SAT}, \quad (11)$$

where: 1) all latitude and longitude values are in minutes of arc, 2) $d(p_c-p_o)$ is the distance in nautical miles between the pixel containing the control point and the subsatellite point, 3) $\bar{L}$ is the mid-latitude of the portion of the Landsat scene in which control points lay, and 4) ϕ_{SAT} is the inclination of the scan line of the MSS aboard the Landsat-1 satellite, as measured counter-clockwise from the equator.

The control points (and hence the subsatellite points) were selected to extend as far as possible across that portion of the scene from which depth information would be taken. It was not necessary to select points from over the entire scene, since any geometric inaccuracies within the scene would be expected to increase with distance. It was, however, necessary to extend the selection of the control points beyond the boundaries of the testing areas (less than .1 nautical mile in either case) to procure a sufficient number of reliable points.

Step 2.

To test the accuracy of the navigation algorithm, the "ground control set" from each scene was further divided into two sample sets: a) a test sample set containing those points from which the coordinates of the reserve sample points would be calculated and b) a reserve control sample with which to test location accuracies. Given the line number and pixel number of each reserve sample point, coordinates were calculated from each of the two ground control points within the sample as:

$$LAT(P,\ell) = LAT(P_0,\ell) - d(P-P_0)\,SIN\,\phi_{SAT}, \tag{12}$$

$$LONG(P,\ell) = LONG(P_0,\ell) + [d(P-P_0)/COS\,L]\,COS\,\phi_{SAT}, \tag{13}$$

where (P_0,ℓ) is the subsatellite point of the scan line containing the reserve point (calculated in an intermediate step).

In both equations, the first term is the previously calculated latitude/longitude of the control sample point, the second term accounts for the change in subsatellite latitude/longitude with change in scan line, and the last term then accounts for the change in latitude/longitude with displacement along a particular scan line.

The circular errors in location (at the 90 percent level) (Bowditch, 1977), were 113.3m based on six reserved control points for the Bahama Test Area, and 143.5m based on five reserved control points for the Florida Test Area.

LIST OF REFERENCES

Austin, R. W. 1974. The remote sensing of spectral radiance from below the ocean surface. Optical Aspects of Oceanography. (Jerlov, N. G., and E. S. Nielson, editors). London: Acedemic Press.

Bowditch, N. 1977. American Practical Navigator (Vol I). Suitland: Defense Mapping Agency Hydrographic Center, 1386 p.

Brown, W. L., F. C. Polycn, A. N. Sellman, 1971. Water Depth Measurement by Wave Refraction and Multispectral Techniques (Report No. 31650-31T). Ann Arbor: Willow Run Laboratories, 54 p.

Cox, C. and W. Munk. 1954. Measurement of the roughness of the sea surface from photographs of the sun's glitter. Journal of the Optical Society of America, 44:838 - 850.

Defense Mapping Agency Hydrographic/Topographic Center. 1980. Organization and Function Manual, Washington, DC.

Defense Mapping Agency Hydrographic/Topographic Center. 1984. Panel presentation delivered by Dr. Kenneth Daugherty, Technical Director DMAHTC, at Pacific Conference on Marine Technology, Honolulu.

Gordon, H. R., D. K. Clark, J. W. Brown, O. B. Brown, R. H. Evans, and W. W. Broenkow. 1983. Phytoplankton pigment concentrations in the Middle Atlantic Bight: Comparison of ship determinations and CZCS estimates. Applied Optics. 22:20.

Halperin, M., et al. 1955. Tables of percentage points for the studentized maximum absolute deviation in normal samples. American Statistical Association Journal. 50(269):185 - 195.

Hammack, J. 1977. Landsat goes to sea. Photogrammetric Engineering and Remote Sensing, 43(6):683 - 691.

Hammack, J. 1981. Personal Communication.

Hasell, P. G. Jr., et al. 1977. Active and Passive Multi-spectral Scanner for Earth Resources Applications on Advanced Applications Flight Experiment, Report No.115000-49-F. Ann Arbor: Environmental Research Institute of Michigan.

Jerlov, N. G. 1976. Marine Optics. Amsterdam: Elsevier Scientific Publishing Company, 231 p.

Joy, R. T. 1981. Proposed Standard Operating Procedures for Preparing Landsat Zoned-depth Manuscripts in Support of NAVOCEANO Pre-survey Planning. Unpublished report, Washington, DC: Defense Mapping Agency, Hydrographic/Topographic Center, 21 p.

Lodge, D. W. S. 1983. Expressions of bathymetry on SEASAT Synthetic radar images. In: Satellite Microwave Remote Sensing (T. D. Allan, ed). Chichester: Ellis Horwood, LTD, 526 p.

Lyzenga, D. R., and F. C. Polycn 1979. Techniques for the Extraction of Water Depth Information from Landsat Digital Data. Ann Arbor: Environmental Research Institute of Michigan, 57 p.

Lyzenga, D. R. 1981. Remote Sensing of Bottom Reflectance and Water Attenuation Parameters in Shallow Water Using Aircraft and Landsat Data. International Journal of Remote Sensing. 2(1):71 - 82.

NASA/Goddard Space Flight Center. 1982. Personal Communications with Landsat project personnel.

Polcyn, F. C., and D. Lyzenga. 1975. Remote Bathymetry and Shoal Detection with ERTS (final report). 54 p. Ann Arbor: Environmental Research Institute of Michigan.

Polcyn, F. C. 1976. NASA/Cousteau Ocean Bathymetry Experiment (final report). Ann Arbor Environmental Research Institute of Michigan, 132 p.

Polcyn, F. C., D. R. Lyzenga and, F. J. Tanis 1977. Demonstration of Satellite Bathymetric Mapping (final report). Ann Arbor: Environmental Research Institute of Michigan.

Slater, P. N. 1980. Remote Sensing. Reading:Addison-Wesley Publishing Company. 547 p.

Taranik, J. V. 1978. Characteristics of the Landsat Multispectral Data System. Sioux Falls: U.S. Geological Survey, 76 p.

U.S. Geological Survey. 1979. Landsat Data User's Handbook. Sioux Falls: U.S. Geological Survey.

Umbach, M. J. 1976. Hydrographic Manual. Rockville: National Oceanic and Atmospheric Administration, 307 p.

Warne, D. K. 1978. Landsat Image Analysis: Application to Hydrographic Mapping. Ph. D. Thesis, Australian National University, Canberra, ACT., Australia, 217 p.

INITIAL DISTRIBUTION LIST

		No.Copies
1.	Defense Technical Information Center Cameron Station Alexandria, VA 22314	2
2.	Library, Code 0142 Naval Postgraduate School Monterey, CA 93943	2
3.	Chairman (Code 68Mr) Department of Oceanography Naval Postgraduate School Monterey, CA 93943	1
4.	Chairman (Code 63Rd) Department of Meteorology Naval Postgraduate School Monterey, CA 93943	1
5.	Dr. James L. Mueller (Code 68My) Department of Oceanography Naval Postgraduate School Monterey, CA 93943	3
6.	Richard T. Joy DMA Hydrographic/Topographic Center Code TOCT Washington, DC 20315	3
7.	Director Naval Oceanography Division Naval Observatory 34th and Massachusetts Avenue, NW Washington, DC 20390	1
8.	Commander Naval Oceanography Command NSTL Station Bay St. Louis, MS 39522	1
9.	Commanding Officer Naval Oceanographic Office NSTL Station Bay St. Louis, MS 39522	1
10.	Commanding Officer Fleet Numerical Oceanography Center Monterey, CA 93940	1

11. Commanding Officer — 1
Naval Ocean Research and Development Activity
NSTL Station
Bay St. Louis, MS 39522

12. Commanding Officer — 1
Naval Environmental Prediction Research Facility
Monterey, CA 93940

13. Chairman, Oceanography Department — 1
U.S. Naval Academy
Annapolis, MD 21402

14. Chief of Naval Research — 1
800 N. Quincy Street
Arlington, VA 22217

15. Office of Naval Research (Code 420) — 1
Naval OCean Research and Development Activity
800 N. Quincy Street
Arlington, VA 22217

16. Scientific Liaison Office — 1
Office of Naval Research
Scripps Institution of Oceanography
La Jolla, CA 92037

17. Library — 1
Scripps Institution of Oceanography
P. O. Box 2367
La Jolla, CA 92037

18. Library — 1
Department of Oceanography
University of Washington
Seattle, WA 98105

19. Library — 1
CICESE
P. O. Box 4803
San Ysidro, CA 92073

20. Library — 1
School of Oceanography
Oregon State University
Corvallis, OR 97331

21. Commander 1
Oceanographic Systems Pacific
Box 1390
Pearl Harbor, HI 96860

22. Director 1
Defense Mapping Agency
Code PPH
Bldg. 56, U.S. Naval Observatory
Washington, DC 20305

23. Director 1
DMA Hydrographic/Topographic Center
Code HO
Washington, DC 20315

210277

Thesis
J842 Joy
c.1 An assessment of the potential role of multi-spectral imagery in bathymetric charting.